Contrails

FOREWORD

This work was conducted by the National Carbon Company, A Division of Union Carbide Corporation, under USAF Contract AF 33(616)-6915. This contract was initiated under Project No. 7350 "Refractory Inorganic Non-Metallic Materials," Task No. 735002 "Refractory Inorganic Non-Metallic Materials: Graphitic;" Project No. 7381 "Materials Application," Task No. 738102 "Materials Process;" and Project No. 7-817 "Process Development for Graphite Materials." The work was administrated under the direction of the AF Materials Laboratory, Aeronautical Systems Division, with Captain R. H. Wilson, L. J. Conlon and W. P. Conrardy acting as Project Engineers.

Work under this contract has been in progress since May 1, 1960. The work covered in this report was conducted at the Research Laboratory of the National Carbon Company located at Parma 30, Ohio, under the direction of J. C. Bowman, Director of Research, and W. P. Eatherly, Assistant Director of Research.

It is a pleasure to thank J. A. Krumhansl, J. W. McClure, and Charles S. Smith for helpful discussions and R. Moyer for programming the numerical computations for the RPC-4000 electronic computer. The author apologizes for any omissions he may have made in surveying the literature of important measurements of the specific heat of graphite and would appreciate having such omissions brought to his attention.

Other reports issued under USAF Contract AF 33(616)-6915 have included:

WADD Technical Notes 61-18 and 61-18, Part II, progress reports covering work from the start of the Contract on May 1, 1960 to October 15, 1961, and the following volumes of WADD Technical Report 61-72 covering various subject phases of the work:

Volume I	Observations by Electron Microscopy of Dislocations in Graphite, by R. Sprague.
Volume II	Applications of Anisotropic Elastic Continuum Theory to Dislocations in Graphite, by G. B. Spence.
Volume III	Decoration of Dislocations and Low Angle Grain Boundaries in Graphite Single Crystals, by R. Bacon and R. Sprague.
Volume IV	Adaptation of Radiographic Principles to the Quality Control of Graphite, by R. W. Wallouch.
Volume V	Analysis of Creep and Recovery Curves for ATJ Graphite, by E. J. Seldin and R. N. Draper.
Volume VI	Creep of Carbons and Graphites in Flexure at High Temperatures, by E. J. Seldin.

Approved for Public Release

Contrails

Volume VII	High Density Recrystallized Graphite by Hot Forming, by E. A. Neel, A. A. Kellar, and K. J. Zeitsch.
Volume VII Supplement	High Density Recrystallized Graphite by Hot Forming, by G. L. Rowe and M. B. Carter.
Volume VIII	Electron Spin Resonance in Polycrystalline Graphite, by L. S. Singer and G. Wagoner.
Volume IX	Fabrication and Properties of Carbonized Cloth Composites, by W. C. Beasley and E. L. Piper.
Volume X	Thermal Reactivity of Aromatic Hydrocarbons, by I. C. Lewis and T. Edstrom.
Volume X Supplement	Thermal Reactivity of Aromatic Hydrocarbons, by I. C. Lewis and T. Edstrom.
Volume XI	Characterization of Binders Used in the Fabrication of Graphite Bodies, by E. de Ruiter, A. Halleux, V. Sandor, H. Tschamler.
Volume XI Supplement	Characterization of Binders Used in the Fabrication of Graphite Bodies, by E. de Ruiter, J. F. M. Oth, V. Sandor, and H. Tschamler.
Volume XII	Development of an Improved Large Diameter Fine Grain Graphite for Aerospace Applications, by C. W. Waters and E. L. Piper.
Volume XII Supplement	Development of an Improved Large Diameter Fine Grain Graphite for Aerospace Applications, by R. L. Racicot and C. W. Waters
Volume XIII	Development of a Fine-Grain Isotropic Graphite for Structural and Substrate Applications, by R. A. Howard and E. L. Piper.
Volume XIII Supplement	Development of a Fine-Grain Isotropic Graphite for Structural and Substrate Applications, by R. A. Howard and R. L. Racicot.
Volume XIV	Study of High Temperature Tensile Properties of ZTA Grade Graphite, by R. M. Hale and W. M. Fassell, Jr.
Volume XV	Alumina-Condensed Furfuryl Alcohol Resins, by C. W. Boquist, E. R. Nielsen, H. J. O'Neil, and R. E. Putcher.
Volume XVI	An Electron Spin Resonance Study of Thermal Reactions of Organic Compounds, by L. S. Singer and I. C. Lewis.

Approved for Public Release

Contrails

Volume XVII	Radiography of Carbon and Graphite, by T. C. Furnas, Jr. and M. R. Rosumny.
Volume XVIII	High Temperature Tensile Creep of Graphite, by E. J. Seldin.
Volume XIX	Thermal Stresses in Anisotropic Hollow Cylinders, by Tu-Lung Weng.
Volume XX	The Electric and Magnetic Properties of Pyrolytic Graphite, by G. Wagoner and B. H. Eckstein.
Volume XXI	Arc Image Furnace Studies of Graphite, by M. R. Null and W. W. Lozier.
Volume XXII	Photomicrographic Techniques for Carbon and Graphite, by G. L. Peters and H. D. Shade.
Volume XXIII	A Method for Determining Young's Modulus of Graphite at Elevated Temperatures, by S. O. Johnson and R. B. Dull.
Volume XXIV	The Thermal Expansion of Graphite in the c-Direction, by C. E. Lowell.
Volume XXV	Lamellar Compounds of Nongraphitized Petroleum Cokes, by H. F. Volk.
Volume XXVI	Physical Properties of Some Newly Developed Graphite Grades, by R. B. Dull.
Volume XXVII	Carbonization Studies of Aromatic Hydrocarbons, by I. C. Lewis and T. Edstrom.
Volume XXVIII	Polarographic Reduction of Polynuclear Aromatics, by I. C. Lewis, H. Leibecki, and S. L. Bushong.
Volume XXIX	Evaluation of Graphite Materials in a Subscale Solid Propellant Rocket Motor, by D. C. Hiler and R. B. Dull.
Volume XXIX Supplement	Evaluation of Graphite Materials in a Subscale Solid Propellant Rocket Motor, by S. O. Johnson and R. B. Dull.
Volume XXX	Oxidation Resistant Graphite Base Composites, by K. J. Zeitsch and J. Criscione.
Volume XXXI	High Performance Graphite by Liquid Impregnation, by C. E. Waylett, M. A. Spring, and M. B. Carter.
Volume XXXII	Studies of Binder Systems for Graphite, by T. Edstrom, I. C. Lewis, R. L. Racicot, and C. F. Stout.
Volume XXXIII	Investigation of Hot Worked Recrystallized Graphites, by J. H. Turner and M. B. Carter.

Approved for Public Release

Contrails

Approved for Public Release

Contrails

ABSTRACT

A literature survey was made of the experimental values of the specific heat of graphite. Most of the measurements from 20°K to 3800°K were reanalyzed and a new average curve is given for each experimental run. Some of the new curves are significantly different from the original curves. Estimates are given of the C_p-C_v term, the electronic specific heat, and the specific heat of the lattice vibrations. The lattice specific heat was approximated by various combinations of Einstein and one- and two-dimensional Debye functions. The characteristic temperatures were selected by a least-squares curve-fitting procedure.

This report has been reviewed and is approved.

W. G. RAMKE
Chief, Ceramics and Graphite Branch
Metals and Ceramics Division
AF Materials Laboratory

Approved for Public Release

Contrails

TABLE OF CONTENTS

Approved for Public Release

Contrails

LIST OF ILLUSTRATIONS

Approved for Public Release

Contrails

LIST OF TABLES

Approved for Public Release

Contrails

1. INTRODUCTION

This report gives the results of a literature survey of the experimental values of the specific heat of graphite and the results of attempts to approximate the lattice specific heat by relatively simple analytic functions. The survey covers most of the experimental values of the specific heat at constant pressure C_p from 20 to 3800°K. The lattice specific heat C_ℓ is estimated by subtracting from the average experimental values of C_p an estimate of the thermodynamic formula for $(C_p - C_v)$ and an estimate of the specific heat of the electrons C_e. The lattice specific heat was approximated by various combinations of Einstein and one- and two-dimensional Debye functions. The Debye or characteristic temperatures were selected by a least-squares curve-fitting program on an electronic computer.

Several of the existing literature surveys [1-8] of thermal properties include the specific heat of graphite. The present study differs from these in two important respects. First, the original experimental data have been reanalyzed, whenever possible, and an average specific heat curve obtained for each sample measured. Second, these average specific heat curves for individual samples are presented in tabular and graphical forms which permit an evaluation of the experimental uncertainty in the average specific heat for all samples and which show to what extent the specific heat differs for different types of graphite. The original experimental data were reanalyzed for several reasons, the simplest being to provide a check against numerical errors in data reduction. Much of the early literature gave the mean specific heat over large temperature intervals. In these cases the true specific heat at each temperature has been calculated from the original enthalpy measurements. Some of the recent literature report specific heat curves with sharp bends or with sections which decrease with increasing temperature. Such behavior seems unlikely and appears to the present author to be due to the manner by which the specific heat was obtained from the enthalpy measurements. The total specific heat function is the sum of six complicated analytic functions representing the contributions of the six branches of the frequency distribution in $\vec{k}$ space. It appears to be impossible to accurately represent the specific heat function over a several hundred degree temperature interval by only 2 or 3 terms of a power series expansion in the temperature. On the other hand, when more terms are used and the coefficients are determined by a least-squares curve fitting to the experimental enthalpy data, then in practice the resulting curve tends to follow small drifts in the data which result in the erroneous features of the specific heat curve mentioned above. Consequently, it appears that "best by eye" curve fitting yields all the accuracy which can be obtained in most cases, and this method has been used exclusively in this work.

For many purposes it is sufficient to have the empirical specific heat curve in tabular form. However, for certain theoretical studies and for some computer numerical computations it is more convenient to represent the empirical specific heat curve by an analytic function. In 1923 Magnus [9] used

Manuscript released by the author June 1963 for publication as an ASD Technical Documentary Report.

Approved for Public Release

Contrails

a sum of two three-dimensional Debye functions with Debye temperatures of 760 and 2280°K to approximate the specific heat curve. The analytical and empirical curves crossed at several temperatures but between these temperatures the difference was usually much larger than the experimental uncertainty in the empirical curve. Later it was recognized that, because of the weak binding between layers, graphite should resemble a two-dimensional crystal and its specific heat might be better approximated by two-dimensional Debye functions, for which the specific heat is proportional to T^2 at low temperatures. Still later Krumhansl and Brooks [10] pointed out that, as the temperature approaches the absolute zero, the T^2 variation must change to a T^3 variation. The trend of the specific heat curve in this transition region is now satisfactorily understood from the results of a number of theoretical calculations [11] but the actual formulas are rather complicated. Since the objective of the present work is to get tractable formulas to approximate the specific heat at higher temperatures where the magnitude of the specific heat is large, no attempt has been made to fit the specific heat curve below 20°K. The frequency distributions of the acoustical modes have been approximated by the triangular two-dimensional Debye distributions, those of the optical modes by peaked Einstein distributions or by rectangular distributions constructed from one-dimensional Debye distributions. In a few cases the optical modes were omitted or, more exactly, were assumed to have the same frequency distribution as the acoustical modes. It should be noted that Tarasov [12] has approximated the specific heat in the low temperature transition region by a combination of two- and three-dimensional Debye functions. Although it gives a $T^2 \rightarrow T^3$ transition, it is otherwise inadequate in that it fails to take into account the differences between the various acoustical and optical modes.

Approved for Public Release

Contrails

2. LITERATURE SURVEY

2.1. Method of Evaluation

The following procedures were used in reanalyzing the original data reported on measurements of the specific heat. If the enthalpy (total heat content) was measured by, say, dropping a hot sample into a cold calorimeter, then the experimental enthalpy points were plotted against the temperature on large graph paper. A "best by eye" smooth curve was drawn through these points. The specific heat at constant pressure was obtained from the slopes of tangents to the enthalpy curve at a standard set of temperatures. Since there is always some error in determining the slopes of tangents to a graphical curve, these C_p values were plotted against the temperature and a "best by eye" smooth curve drawn through them. This smooth curve was taken as the average specific heat of the sample, and the reported tabular values are the coordinates of this curve. In some cases it was felt that the scatter in the enthalpy points at the higher temperatures made it impossible to adequately determine a smooth curve. Such regions were omitted and results are given here for a smaller temperature interval than in the original report.

If the specific heat was measured by, say, adding a small amount of heat to a sample at temperature, then the experimental C_p points were plotted against the temperature. A "best by eye" smooth curve was drawn through these points, and the coordinates of this curve at the standard set of temperatures are given in the tables. Differences between the smooth curve reported here and the smooth curve reported in the original article must be ascribed to differences in taste as to how to fit the curve. The present author does not claim that his curve is more accurate than that of the original experimentalist, but the differences form some indication of the uncertainty in the coordinates of the smooth curve.

At certain temperatures, the choice of which depended on the nature of the experimental curve, a rough estimate of the error ΔC_p has been made. This estimate is never less than the originally reported error and is greater than the reported error whenever the scatter in the experimental points was so large that the average specific heat curve could not be determined within the original reported error. Although the quantity ΔC_p was not calculated from a precise statistical formula, it is intended that it represents limits such that there is about a 50 per cent probability that the true value lies within the range $C_p \pm \Delta C_p$. The temperatures at which the error was estimated were chosen so that ΔC_p should vary monotonically between these temperatures.

2.2. Summary of Experimental Measurements of the Specific Heat at Constant Pressure

In the following, individual samples are designated by two sets of symbols, such as CeNG-D55. The first set (CeNG) identifies the type of graphite (Ceylon natural graphite) and the second set (D55) identifies the author and year of publication (De Sorbo, 1955). The explanation of these symbols and the key to the literature references are given in Table 1.

Approved for Public Release

Contrails

Table 1. Explanation of Sample Designation

Symbol	Type of Graphite	First Author	Reference No.
CeNG - D55	Ceylon natural graphite	De Sorbo	13
CS - D53	National Carbon Co. grade CS	"	14
Reac - B54	A.E.R.E. reactor graphite	Bergenlid	15
AGOT - E45	National Carbon Co. grade AGOT (Data represent an average of 7 unirradiated samples)	Estermann	16
Fab - J34	National Carbon Co. fabricated	Jacobs	17
Fab - N11	Fabricated graphite	Nernst	18
Fab - K11	Fabricated graphite	Koref	19
CeNG - M23	Ceylon natural graphite	Magnus	9
Unk - W75	Unknown	Weber	20
CeRt - S24	Ceylon natural and "retort" graphite	Schläpfer	21
7087 - L56	Speer Carbon Co. grade 7087	Lucks	22
GBH - L56	National Carbon Co. grade GBH	"	22
ATJ - N60	National Carbon Co. grade ATJ	Neel	23
ATJ - F60	National Carbon Co. grade ATJ	Fieldhouse	24
GBE - F56	National Carbon Co. grade GBE	"	25
3474 - F56	Speer Carbon Company grade 3474	"	25
CaFi - W17	Carbon lamp filament	Worthing	26
GBH - R57	National Carbon Co. grade GBH	Rasor	27
GBE - R57	National Carbon Co. grade GBE	"	27
3474 - R57	Speer Carbon Co. grade 3474	"	27
7087 - R57	Speer Carbon Co. grade 7087	"	27

Approved for Public Release

Contrails

Table 2 gives the results of the reanalysis of the experimental measurements of the specific heat at constant pressure. For brevity the estimated error ΔC_p is given as a per cent of C_p. In two cases, only a few measurements were made and a smooth curve could not be determined. In these cases the measurements at temperature are reported. It is impossible to adequately present all the data of Table 2 in a single small graph. Figures 1 and 2 show all the measurements in the temperature ranges 200 to 460°K and 1000 to 2000°K.

The extent to which the specific heat is different for different types of graphite cannot be satisfactorily determined from the present data. It is known[28] that below 20°K the specific heat of natural single-crystal graphite is slightly less and that of lampblack-based and turbostratic pyrolytic graphite is slightly greater than that of a good quality coke-based graphite. DeSorbo's results,[13] shown in part in Figure 1, indicate that the specific heat of Ceylon natural graphite is as much as 9 per cent less than that of artificial graphite in the temperature interval 120 to 300°K. This difference is over twice as large as the combined experimental errors of the two curves. Above 300°K the measurements on natural and fabricated graphite do not seem to be significantly different. Also, the difference between the specific heat of different grades of graphite seems to be about the same as the difference between various measurements of the same grade of graphite. This may be seen, for example, by comparing the results for grades ATJ and GBH (grade GBH should have identically the same thermal properties as grade ATJ) with the results for other grades. It appears that within the accuracy of the present measurements the specific heat of all coke-based artificial graphites is the same at all temperatures above a few degrees absolute.

Table 3 gives the average specific heat at constant pressure for all coke-based graphites. Below 300°K this curve is based on the individual measurements of only coke-based graphites. Above 300°K it is based on the data for all graphites. The average curve is shown as a dotted line in Figures 1 and 2 and represents a "best by eye" fit of the individual measurements on graphs covering the entire temperature range with proper consideration given to the probable errors of the individual curves. The quantity ΔC given in Table 3 is an estimated error such that most of the reliable individual measurements fall within the range $C_p \pm \Delta C$. The subscript "p" is omitted since ΔC is also the probable error of the specific heat at constant volume and of the lattice specific heat.

Table 3 also gives the estimated values of the lattice specific heat C_l, of the difference $(C_p - C_v)$ between the specific heats at constant pressure and at constant volume, of the specific heat C_e of the electrons, and of the contribution C_t of a thermally activated process, possibly the creation of vacancies, which occurs at very high temperatures. These quantities are important for the theoretical interpretation of the specific heat of graphite and are discussed further in the following sections.

2.3. Difference $(C_p - C_v)$ of the Specific Heats

The difference between the specific heat at constant pressure and the specific heat at constant volume is given by the well-known thermodynamic formula

Approved for Public Release

Contrails

Table 2. Specific Heat at Constant Pressure for Various Types of Graphite

(Part 1)

T °K	CeNG - D55 C_p	ΔC_p	CS - D53 C_p	ΔC_p	Reac - B54 C_p	ΔC_p	AGOT - E45 C_p	ΔC_p	Fab - J34 C_p	ΔC_p
20	0.0174	5	0.0198	3	0.0178	2	0.0187	3		
25	0.0261		0.0301		0.0289		0.0298			
30	0.0406		0.0441	2	0.0422		0.045			
35	0.0575	4	0.0609		0.0590		0.063			
40	0.0765		0.0795		0.0786		0.082			
45	0.0965		0.0987		0.1003		0.103			
50	0.119		0.118		0.123		0.127			
55	0.143		0.141		0.147		0.153			
60	0.168		0.165		0.173		0.179			
65	0.195	2	0.191		0.198		0.206			
70	0.223		0.219		0.225		0.234			
75	0.252		0.249		0.252		0.262			
80	0.280		0.279		0.280		0.291			
85	0.309		0.309		0.309		0.321			
90	0.339		0.341		0.338	1	0.351		0.333	1
95	0.369		0.373				0.381		0.363	
100	0.400	1.5	0.405	1			0.412		0.395	
110	0.462		0.472				0.475	3	0.463	
120	0.525		0.541						0.535	
130	0.592		0.613						0.609	
140	0.659		0.692						0.686	
150	0.729		0.775						0.766	
160	0.799		0.859						0.849	
170	0.871	1	0.943						0.934	
180	0.945		1.028						1.019	
190	1.021		1.112						1.106	
200	1.097		1.197	0.7					1.193	
210	1.173		1.282						1.279	
220	1.251		1.367						1.368	
230	1.329		1.453						1.456	
240	1.409		1.539						1.545	
250	1.488	1	1.625						1.635	
260	1.567		1.712						1.725	
270	1.646		1.800						1.815	
280	1.725		1.887						1.903	
290	1.804		1.973						1.990	
300	1.883	2	2.060	1					2.075	1

Units: C_p - cal/mole °K; ΔC_p - per cent of C_p

Approved for Public Release

Contrails

Table 2. Specific Heat at Constant Pressure for Various Types of Graphite

(Part 2)

T °K	Fab - N11 C_p	Fab - N11 ΔC_p	Fab - K11 C_p	Fab - K11 ΔC_p
82.5	0.29			
87.5	0.32			
137.9			0.676	
231.4			1.484	
235.3			1.506	

Units: C_p - cal/mole °K; ΔC_p - per cent of C_p

(Part 3)

T °K	CeNG - M23 C_p	CeNG - M23 ΔC_p	Unk - W75 C_p	Unk - W75 ΔC_p	CeRt - S24 C_p	CeRt - S24 ΔC_p
300	1.83	10	2.11	2	2.09	5
350	2.40		2.56		2.53	
400	2.91	5	2.98		2.91	1
450	3.28		3.36		3.27	
500	3.58	2	3.69		3.58	
550	3.82		3.98		3.85	
600	4.03	1	4.21	3	4.08	
650	4.23				4.28	
700	4.41		4.58	?	4.46	
750	4.58				4.59	
800	4.74		4.82	3	4.71	
850	4.88		4.89		4.81	
900	5.00		4.95		4.89	
950	5.09		5.01		4.97	
1000	5.17		5.06		5.04	
1050	5.24	1	5.10		5.11	
1100	5.30		5.14		5.17	
1150	5.34		5.18		5.23	
1200	5.37	2	5.22		5.29	
1250			5.25		5.35	
1300			5.28		5.40	
1350			5.31		5.45	
1400			5.34	2	5.50	1

Units: C_p - cal/mole °K; ΔC_p - per cent of C_p

Approved for Public Release

Table 2. Specific Heat at Constant Pressure for Various Types of Graphite

(Part 4)

T °K	7087 - L56 C_p	ΔC_p	GBH - L56 C_p	ΔC_p	ATJ - N60 C_p	ΔC_p	ATJ - F60 C_p	ΔC_p	GBE - F56 C_p	ΔC_p	3474 - F56 C_p	ΔC_p	CaFi - W18 C_p	ΔC_p
300	1.77	2	2.25	2										
400	2.71		2.88											
500	3.59		3.45		3.20	10								
600	4.15		3.91		3.76									
700	4.48		4.28		4.23		4.32	3						
800	4.71		4.56		4.60		4.57		4.28	3	4.36	3		
900	4.91		4.77		4.86		4.80		4.71		4.75			
1000	5.09	3	4.93	3	5.02		5.02		5.08		5.10			
1100	5.25		5.06		5.14		5.20		5.38		5.33			
1200	5.41		5.18		5.24		5.34		5.56		5.48		5.55	5
1300	5.55		5.29		5.32		5.46		5.66	3	5.57		5.60	
1400	5.67		5.39		5.40	5	5.56		5.74		5.64		5.65	
1500	5.79		5.48				5.64		5.80	5	5.70		5.70	
1600	5.90		5.58				5.73				5.76	3	5.75	
1700	6.01		5.67				5.81						5.80	
1800	6.10		5.76				5.88	3					5.85	
1900	6.19		5.84										5.90	
2000	6.27	5	5.93	5									5.95	

Units: C_p - cal/mole °K; ΔC_p - per cent of C_p

Approved for Public Release

Contrails

Table 2. Specific Heat at Constant Pressure for Various Types of Graphite

(Part 5)

T °K	GBH - R57 C_p	GBH - R57 ΔC_p	GBE - R57 C_p	GBE - R57 ΔC_p	3474 - R57 C_p	3474 - R57 ΔC_p	7087 - R57 C_p	7087 - R57 ΔC_p
1400			5.37	10			5.56	10
1500	5.78	5	5.45		5.53	8	5.70	
1600	5.89		5.52		5.66		5.82	
1700	5.98		5.58		5.76	5	5.93	
1800	6.06		5.64	5	5.83		6.03	5
1900	6.13		5.70		5.89		6.12	
2000	6.19		5.75		5.94		6.21	
2200	6.28		5.84		6.01		6.34	
2400	6.35		5.92		6.05		6.44	
2600	6.41		5.99		6.10		6.53	
2800	6.46		6.05		6.15		6.60	
3000	6.51		6.12		6.22		6.66	
3200	6.58		6.21		6.32		6.72	
3400	6.71		6.35		6.49		6.81	
3500	6.86		6.50		6.63		6.92	
3600	7.22	5	6.78	5	6.83	5	7.10	5
3700	7.86		7.31		7.18		7.44	
3800	8.86		8.43	10	7.80		8.06	
3900	11.7	10			9.2	10	9.9	10

Units: C_p - cal/mole °K; ΔC_p - per cent of C_p

Approved for Public Release

Contrails

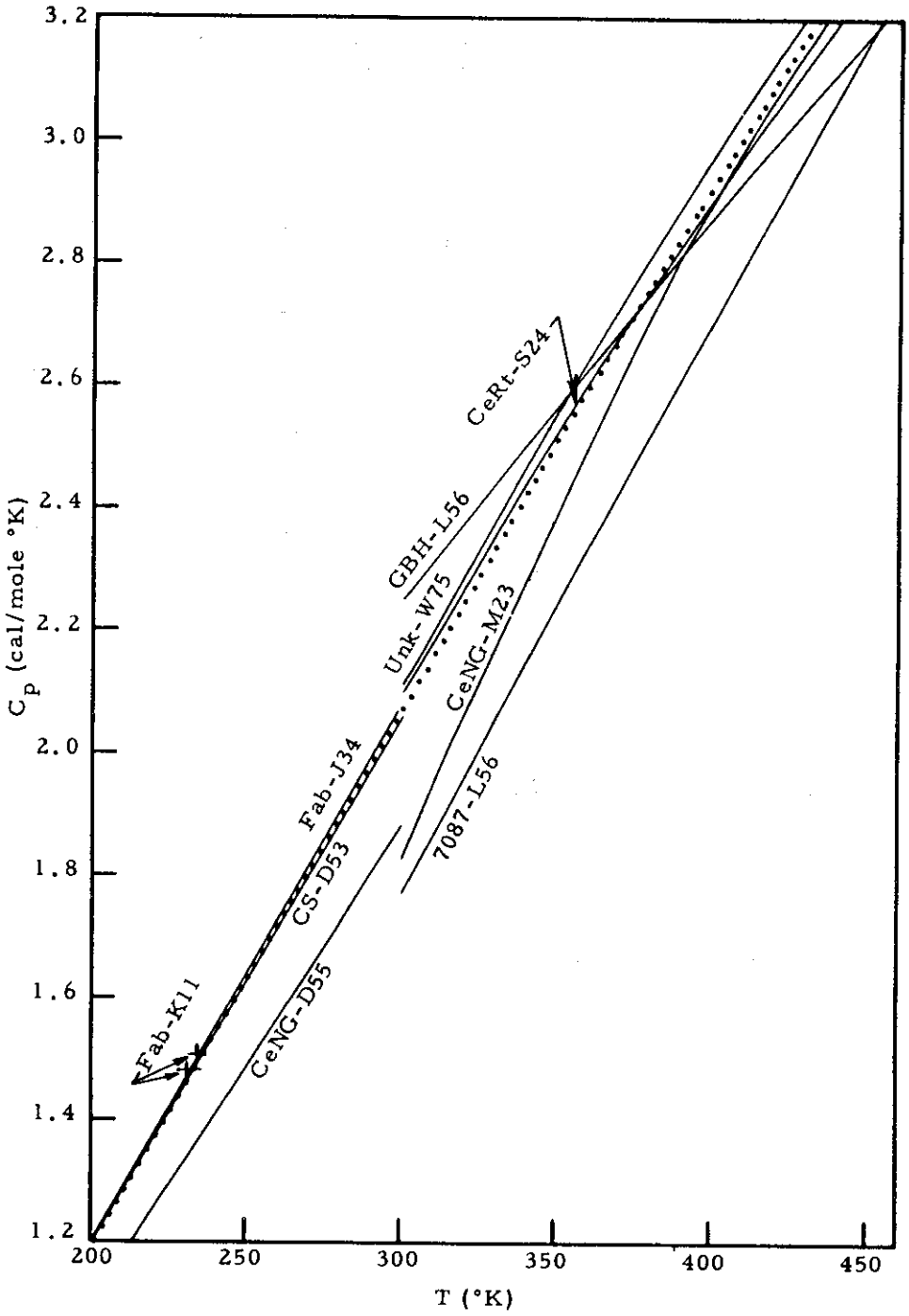

N-4454

Figure 1. Survey of the Specific Heat at Constant Pressure from 200 to 460°K

Approved for Public Release

Contrails

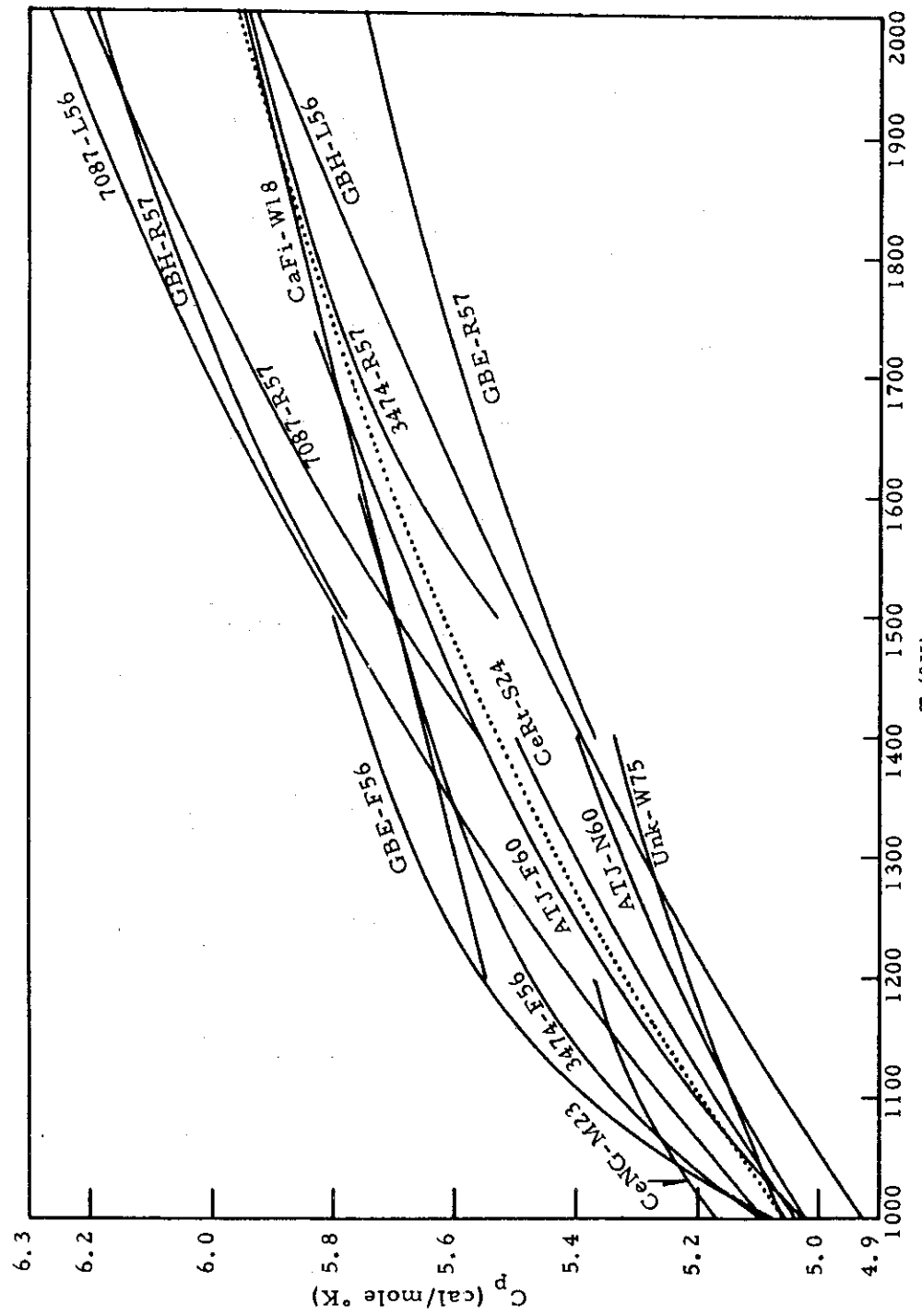

N-4212

Figure 2. Survey of the Specific Heat at Constant Pressure from 1000 to 2000°K

Approved for Public Release

Table 3. Average Values of C_p and ΔC and Estimated Values of C_l, (C_p-C_v), C_e, and C_t for Fabricated Graphite

T	C_p	ΔC	C_l	(C_p-C_v)	C_e	T	C_p	ΔC	C_l	(C_p-C_v)	C_e	C_t
0	0.0	0.0	0.0	0.0		650	4.28	0.11	4.25	0.023	0.0034	
20	0.178	0.0009	0.0178	0.00000	.00005	700	4.45	0.11	4.42	0.025	0.0038	
25	0.296	0.0010	0.0295	0.00001	.00006	750	4.59	0.12	4.56	0.028	0.0043	
30	0.0432	0.0010	0.0431	0.00002	.00007	800	4.72	0.12	4.69	0.030	0.0048	
40	0.0790	0.0015	0.0788	0.00007	.00010	850	4.83	0.12	4.79	0.033	0.0054	
50	0.121	0.002	0.121	0.00030	.00012	900	4.92	0.12	4.88	0.035	0.0059	
60	0.169	0.003	0.168	0.00059	.00015	950	4.99	0.12	4.95	0.037	0.0066	
70	0.222	0.004	0.221	0.00087	.00018	1000	5.06	0.12	5.01	0.040	0.0072	
80	0.279	0.004	0.278	0.00115	.00021	1100	5.19	0.13	5.14	0.044	0.0086	
90	0.339	0.004	0.337	0.00143	.00024	1200	5.32	0.13	5.26	0.049	0.0102	
100	0.402	0.004	0.400	0.00172	.00027	1300	5.43	0.14	5.36	0.054	0.012	
120	0.538	0.005	0.535	0.0023	.00033	1400	5.53	0.15	5.46	0.058	0.014	
140	0.689	0.007	0.686	0.0029	.00039	1500	5.62	0.16	5.54	0.062	0.016	
150	0.772	0.008	0.768	0.0032	.00043	1600	5.70	0.17	5.62	0.066	0.018	
160	0.856	0.009	0.852	0.0034	.00046	1700	5.77	0.17	5.68	0.070	0.021	
180	1.025	0.010	1.020	0.0041	.00054	1800	5.84	0.18	5.74	0.074	0.023	
200	1.195	0.012	1.190	0.0047	.00061	1900	5.90	0.19	5.80	0.077	0.026	
220	1.368	0.014	1.362	0.0054	.00069	2000	5.96	0.20	5.85	0.080	0.029	
240	1.542	0.015	1.535	0.0061	.00078	2200	6.06	0.22	5.94	0.085	0.036	
250	1.630	0.016	1.623	0.0065	.00082	2400	6.14	0.24	6.01	0.089	0.043	
260	1.718	0.017	1.710	0.0068	.00086	2600	6.20	0.26	6.06	0.092	0.051	
280	1.894	0.019	1.886	0.0076	.00095	2800	6.26	0.28	6.11	0.094	0.059	
300	2.070	0.020	2.061	0.0083	.00105	3000	6.33	0.3	6.16	0.095	0.067	0.008
350	2.51	0.04	2.50	0.0103	.0013	3200	6.44	0.3	(6.23)	0.095	0.077	0.041
400	2.94	0.04	2.93	0.0123	.0016	3400	6.59	0.3	(6.22)	0.093	0.087	0.186
450	3.32	0.05	3.30	0.0144	.0019	3500	6.73	0.3	(6.18)	0.092	0.092	0.37
500	3.64	0.06	3.62	0.017	.0022	3600	6.98	0.3	(6.07)	0.090	0.097	0.72
550	3.88	0.08	3.86	0.019	.0026	3700	7.4	0.4	(5.9)	0.088	0.103	1.32
600	4.09	0.10	4.07	0.021	.0030	3800	8.3	0.5	(5.7)	0.086	0.108	2.4

Units: Temperature - °K, Specific Heats - cal/mole °K

Approved for Public Release

Classified

Contrails

$$C_p - C_v = V\beta^2 B T \quad , \tag{1}$$

where V is the molar volume, β is the volume coefficient of thermal expansion, and B is the bulk modulus. For a porous material such as graphite V, β, and B must be evaluated for the crystals and not for the bulk, porous material. All quantities must be evaluated at the temperature T.

2.3.1. Volume Coefficient of Thermal Expansion and Molar Volume

Let a_1, a_2, a_3 be the lattice constants of the unit cell of any crystal. The linear coefficient of thermal expansion is defined by

$$\alpha_i = \frac{1}{a_i} \left(\frac{da_i}{dT} \right)_p \quad . \tag{2}$$

Integration gives

$$a_i(T) = a_i(T_o) \exp \left[\int_{T_o}^{T} \alpha_i \, dT \right] \quad . \tag{3}$$

The volume of the unit cell is

$$V = k \, a_1 \, a_2 \, a_3 \quad , \tag{4}$$

where k is a numerical constant. It follows from (3) and (4) that

$$V(T) = V(T_o) \exp \left[\int_{T_o}^{T} (\alpha_1 + \alpha_2 + \alpha_3) \, dT \right] \quad . \tag{5}$$

The volume coefficient of thermal expansion is defined by

$$\beta = \frac{1}{V} \left(\frac{dV}{dT} \right)_p \quad . \tag{6}$$

On differentiating (5) and substituting into (6), one obtains

$$\beta = \alpha_1 + \alpha_2 + \alpha_3 \quad . \tag{7}$$

Approved for Public Release

Contrails

This result is rigorously correct. The often made claim that it holds only in the approximation of neglecting certain higher-order terms is an erroneous conclusion based on starting with the formula

$$a_i(T) = a_i(T_o)\,[\,1 + \alpha_i\,(T - T_o)\,]\ , \qquad (8)$$

which is itself only an approximation to the correct formula (3).

If c denotes the interlayer distance in the graphite lattice in Angstrom units ($c \sim 3.36$ A) and a denotes the length of the graphite unit cell in the basal plane in Angstrom units ($a \sim 2.46$ A), then the density of the crystal is given by

$$d = (46.0536/a^2 c)\ \ g/cm^3 \qquad (9)$$

and the crystallite molar volume on the physical scale of atomic weights is given by

$$V = (0.260\,884\ a^2c)\ cm^3/mole\ . \qquad (10)$$

A brief literature survey has been made of the X-ray values of the lattice constants of different types of graphite as a function of temperature. The linear coefficients of thermal expansion were obtained from the slopes of the curves of lattice spacing versus temperature. The c-axis spacing and the coefficient of thermal expansion are definitely different for significantly different types of graphite, such as natural single-crystal, coke-based, and lampblack-based graphites. The a-axis spacing and coefficient of thermal expansion appear to be the same for different types of graphite. From a study of several sources [29-35] average curves of lattice spacings and linear coefficients of thermal expansion have been constructed for natural single-crystal and annealed pyrolytic graphite and for a good quality coke-based graphite with a room temperature c-spacing of 3.360 A. The values, given in Table 4, have been made self-consistent in the sense that a lattice spacing and its coefficient of thermal expansion satisfy equation (3). The coefficient of thermal expansion curves are typical of a class of graphites and the values for individual samples may differ by, say, 10 per cent above 100°K and by a factor of two below 100°K. The data above 2800°K were obtained by a linear extrapolation of the coefficient of thermal expansion curves.

The volume coefficient of thermal expansion of graphite can be calculated from the data of Table 4 and equation (7) with the condition that $\alpha_1 = \alpha_2$, and the molar volume is obtained from equation (10).

2.3.2. Bulk Modulus

The bulk modulus has been measured at room temperature but, so far as the author knows, has not been measured at higher temperatures. An

Approved for Public Release

Contrails

Table 4. Lattice Spacings and Crystallite Coefficients of Thermal Expansion of Natural and Coke-Based Graphites

T	Natural and Coke-Based Graphite		Natural and Pyrolytic Graphite		Coke-Based Graphite	
	a	α_1	c	α_3	c	α_3
0	2.4619	0.00	3.3368	0.0	3.3417	0.0
20	2.4619	- 0.01	3.3368	0.3	3.3417	0.6
40	2.4619	- 0.08	3.3369	5.3	3.3419	6.1
60	2.4619	- 0.15	3.3375	12.8	3.3423	14.2
80	2.4619	- 0.3	3.3385	16.7	3.3437	17.5
100	2.4618	- 0.4	3.3397	18.7	3.3449	19.3
120	2.4618	- 0.6	3.3410	20.1	3.3463	20.7
150	2.4617	- 0.9	3.3431	21.6	3.3485	22.2
200	2.4616	- 1.3	3.3467	23.4	3.3523	24.4
250	2.4614	- 1.5	3.3507	24.8	3.3566	26.0
300	2.4613	- 1.5	3.3550	25.9	3.3610	26.9
350	2.4611	- 1.3	3.3594	26.8	3.3656	27.3
400	2.4609	- 1.1	3.3640	27.3	3.3702	27.6
450	2.4608	- 0.9	3.3686	27.6	3.3749	27.8
500	2.4607	- 0.6	3.3732	27.8	3.3796	27.9
600	2.4606	- 0.2	3.3827	28.0	3.3890	28.0
700	2.4606	+ 0.1	3.3922	28.2	3.3989	28.2
800	2.4607	0.4	3.4018	28.4	3.4082	28.4
900	2.4608	0.6	3.4115	28.6	3.4179	28.6
1000	2.4609	0.8	3.4213	28.9	3.4277	28.9
1200	2.4614	1.1	3.4413	29.5	3.4478	29.5
1400	2.4620	1.3	3.4621	30.5	3.4684	30.1
1600	2.4627	1.4	3.4838	32.1	3.4895	30.6
1800	2.4634	1.5	3.5070	34.3	3.5111	31.0
2000	2.4641	1.5	3.5320	36.7	3.5331	31.5
2200	2.4649	1.5	3.5589	39.1	3.5556	31.9
2400	2.4656	1.5	3.5877	41.5	3.5785	32.2
2600	2.4663	1.5	3.6184	43.9	3.6017	32.6
2800	2.4671	1.5	3.6512	46.3	3.6254	32.9
3000	2.4678	1.5	3.6861	48.7	3.6495	33.3
3200	2.4686	1.5	3.7230	51.1	3.6740	33.7
3400	2.4693	1.5	3.7622	53.5	3.6990	34.0
3600	2.4700	1.5	3.8036	55.9	3.7244	34.4
3800	2.4708	1.5	3.8473	58.3	3.7502	34.8

Units: T - °K; a, c - A; α_1, α_3 - 10^{-6}/°K

Approved for Public Release

Contrails

estimate of its temperature dependence can be made in the following way. The bulk modulus of most materials varies approximately linearly with temperature except near the absolute zero, where it is independent of temperature. Hence, it is reasonable to set

$$B(p_o, T) = B(p_o, T_o) + \left.\frac{\partial B(p_o, T_o)}{\partial T}\right)_p (T - T_o), \tag{11}$$

where p_o and T_o denote atmospheric pressure and room temperature. The temperature derivative can be estimated by a method suggested to me by Charles S. Smith. If we consider that

$$B = B(T, V) ,$$

then

$$dB = \left.\frac{\partial B}{\partial T}\right)_V dT + \left.\frac{\partial B}{\partial V}\right)_T dV$$

and

$$\left.\frac{\partial B}{\partial T}\right)_p = \left.\frac{\partial B}{\partial T}\right)_V + \left.\frac{\partial B}{\partial p}\right)_T \left.\frac{\partial p}{\partial V}\right)_T \left.\frac{\partial V}{\partial T}\right)_p . \tag{12}$$

Using the definition of the bulk modulus,

$$B = -V \left.\frac{\partial p}{\partial V}\right)_T , \tag{13}$$

and the definition (6) of the volume coefficient of thermal expansion, one can write (12) in the form

$$\left.\frac{\partial B}{\partial T}\right)_p = \left.\frac{\partial B}{\partial T}\right)_V - \beta B \left.\frac{\partial B}{\partial p}\right)_T . \tag{14}$$

It has been found that in several materials the first term on the right-hand side is at least a factor of 10 smaller than the second term; and we will make the approximation of setting $(\partial B/\partial T)_V$ equal to zero. The pressure derivative can be calculated from the compressibility data.

Approved for Public Release

Contrails

Bridgman [36] has measured the change in volume of a sample of Ceylon graphite as a function of pressure. However, after cycling the sample to 25,000 kg/cm^2 and back to atmospheric pressure the density was only 2.23 g/cm^3, which corresponds to a porosity of 1.64 per cent. Presumably this porosity decreases as the pressure increases, thereby causing the measured compressibility to be too large by, possibly, 10 per cent. Kabalkina and Vereshchagin [37] have measured the change in c-spacing of both Ceylon and fabricated graphite as a function of pressure. The scatter in their data is large enough to mask any difference between the two types.

The compressibility and its pressure derivative can be related to the change in c-spacing as follows. The linear and volume compressibilities are defined by

$$\chi_1 = -\frac{1}{a}\frac{da}{dp}\Bigg)_T \tag{15}$$

$$\chi_3 = -\frac{1}{c}\frac{dc}{dp}\Bigg)_T \tag{16}$$

$$\chi = -\frac{1}{V}\frac{dV}{dp}\Bigg)_T . \tag{17}$$

Applying these formulas to equation (10), one obtains

$$\chi = 2\chi_1 + \chi_3 . \tag{18}$$

The high pressure X-ray data can be represented by an equation of the form

$$(c_o - c)/c_o = h_1 (p - p_o) + h_2 (p - p_o)^2 , \tag{19}$$

where h_1 and h_2 are constants and c_o is the lattice spacing at atmospheric pressure p_o. Differentiation with respect to p yields

$$\chi_3 (p) = \frac{h_1 + 2 h_2 (p - p_o)}{1 - h_1 (p-p_o) - h_2 (p-p_o)^2} . \tag{20}$$

At $p = p_o$

$$\chi_3 (p_o) = h_1 , \tag{21}$$

Approved for Public Release

Contrails

so h_1 is the linear c-axis compressibility at atmospheric pressure. Differentiation of (20) with respect to the pressure and evaluation at $p = p_o$ yields

$$\left(\frac{\partial \chi_3}{\partial p}\right)_T = h_1^2 + 2h_2 \quad \text{at} \quad p = p_o \quad . \tag{22}$$

From (18)

$$\left(\frac{\partial \chi}{\partial p}\right)_T = 2\left(\frac{\partial \chi_1}{\partial p}\right)_T + \left(\frac{\partial \chi_3}{\partial p}\right)_T \quad . \tag{23}$$

The X-ray data indicate that χ_1 is very small over a large change in pressure, so we will make the approximation of setting $(\partial \chi_1 / \partial p)_T = 0$ and of using (22) to give the value of $(\partial \chi / \partial p)_T$. Finally, the bulk modulus by definition is the reciprocal of the compressibility,

$$B = 1/\chi \quad , \tag{24}$$

from which it follows that

$$\left(\frac{\partial B}{\partial p}\right)_T = -\frac{1}{\chi^2}\left(\frac{\partial \chi}{\partial p}\right)_T \quad . \tag{25}$$

The volume compressibility data can be represented by an equation of the form

$$(V_o - V)/V_o = g_1 (p - p_o) + g_2 (p - p_o)^2 \quad , \tag{26}$$

where g_1 and g_2 are constants. An elementary but tedious analysis indicates that porosity causes a significant change in g_1 and a negligible change in g_2. If $(V_o - V)/V_o (p - p_o)$ and $(c_o - c)/c_o (p - p_o)$ are plotted versus $(p - p_o)$, the results should be straight lines with intercepts at $p = p_o$ of g_1 and h_1 and with slopes of g_2 and h_2. Bridgman's smoothed data give an extremely linear curve out to 15,000 kg/cm^2 and a definite deviation from linearity at higher pressures. The scatter in the original Russian data is too large to confirm the linear variation. A derivation similar to that leading to equation (22) yields

$$\left(\frac{\partial \chi}{\partial p}\right)_T = g_1^2 + 2g_2 \quad \text{at} \quad p = p_o \quad . \tag{27}$$

Approved for Public Release

Contrails

It turns out that g_1^2 and h_1^2 are about a factor of 10 smaller than $2g_2$ and $2h_2$. It follows from this and the approximate equality of the pressure derivatives of χ and χ_3 that g_2 and h_2 are approximately equal and, hence, the slopes of the curves mentioned above should be nearly the same.

Since Bridgman's data cover a much larger pressure range, his results were used to determine g_2; and we make the approximation that $h_2 = g_2$. A "best by eye" line with slope h_2 was drawn through the Russian data and the intercept at $p = p_o$ taken as the value of h_1. The results are

$$\chi_3 = h_1 = (2.70 \pm 0.1) \times 10^{-12} \text{ cm}^2/\text{d} \tag{28}$$

$$h_2 = -(32.71 \pm 0.1) \times 10^{-24} \text{ cm}^4/\text{d}^2 \tag{29}$$

and

$$\left(\frac{\partial \chi_3}{\partial p}\right)_T = -58.1 \times 10^{-24} \text{ cm}^4/\text{d}^2 \quad . \tag{30}$$

The compressibility χ_1 can be roughly estimated from the elastic constants to be

$$\chi_1 = -0.044 \times 10^{-12} \text{ cm}^2/\text{d} \tag{31}$$

with possibly a large but unknown error. From (18) the volume compressibility is found to be

$$\chi = (2.61 \pm 0.1) \times 10^{-12} \text{ cm}^2/\text{d} \quad . \tag{32}$$

From (24) and (25) the bulk modulus and its pressure derivative are calculated to be

$$B = (3.83 \pm 0.1) \times 10^{11} \text{ d/cm}^2 \tag{33}$$

and

$$\left(\frac{dB}{dp}\right)_T = 8.5 \pm 0.6 \; . \tag{34}$$

From (11) and (14) one obtains

$$B = [3.83 - 0.00077\,(T-300)] \times 10^{11} \text{ d/cm}^2 \; , \tag{35}$$

in which T is in °K. Within the accuracy of the present measurements these results apply to both natural and fabricated graphite.

Approved for Public Release

Contrails

2.3.3. Numerical Estimate of (C_p-C_v)

The difference between the specific heats at constant pressure and at constant volume can be calculated from equation (1) and the numerical data given in the previous sections. Of the factors in $V\beta^2BT$, only β depends strongly on the type of graphite. The values of (C_p-C_v) for fabricated graphite are given in Table 3. For comparison a short set of values for natural graphite is given in Table 5. Within a few hundred degrees of room temperature, the values should be correct to within, say, 10 per cent but they may be in error by a factor of about 2 at the higher temperatures due to a failure of formula (11) to hold over such a large temperature interval. Below 1000°K, the difference between the values for natural and fabricated graphite may not be significant. At higher temperatures, the values for natural graphite are definitely greater due to the higher thermal expansion of natural graphite.

Table 5. Average Values of (C_p-C_v) for Natural Graphite

T	(C_p-C_v)	T	(C_p-C_v)
0	0.0	600	0.021
50	0.00020	800	0.030
100	0.00161	1000	0.040
150	0.0029	1200	0.050
200	0.0043	1400	0.060
250	0.0058	1600	0.073
300	0.0076	2000	0.108
350	0.0098	2400	0.147
400	0.0120	3000	0.205
450	0.0141	3400	0.237
500	0.017	3800	0.258

Units: T - °K; (C_p-C_v) - cal/mole °K

In several studies of the specific heat of graphite, the difference (C_p-C_v) has been calculated from the formula

$$C_p-C_v = A\,C_p^2\,T, \tag{36}$$

where A is supposedly a constant which can be calculated from

$$A = V\beta^2\,B\,/\,C_p^2 \tag{37}$$

using room temperature values. The constancy of A can be checked by evaluating the right-hand side of (37) within a few hundred degrees of room temperature, where equation (35) for B should be reliable. The results are given in

Approved for Public Release

Contrails

Table 6 for fabricated graphite. The complete lack of constancy of A can be traced to the fact that C_p decreases to small values at much higher temperatures than does β.

Table 6. Values of $V\beta^2 B / C_p^2$ for Fabricated Graphite

T	$V\beta^2 B/C_p^2$	T	$V\beta^2 B/C_p^2$
50	411	300	6.4
100	106	400	3.6
150	35	500	2.6
200	16	600	2.1
250	9.4	700	1.8

Units: T - °K; $V\beta^2 B / C_p^2$ - 10^{-6} mole/cal

2.4. Electronic Specific Heat

The specific heat of the conduction electrons can be calculated from the electronic band structure of single-crystal graphite under the restriction that the lattice constants or, more precisely, the band parameters do not change with temperature. Komatsu and Nagamiya[38] have derived the basic formula for the electronic specific heat. J. W. McClure has supplied the author with a slightly more accurate version of this formula. McClure further suggests that at very high temperatures the electronic specific heat should approach the values calculated for a purely two-dimensional structure. Therefore, following McClure we take

$$C_e = 3R\,(1.32546)\,(kT/\gamma_0)^2\,(0.5 + 0.096797\,\gamma_1/kT + 0.501557\,kT/\gamma_1) \quad \text{for } T \leq 0.73394\,\gamma_1/k \tag{38}$$

and

$$C_e = 3R\,(1.32546)\,(kT/\gamma_0)^2 \quad \text{for } T \geq 0.73394\,\gamma_1/k, \tag{39}$$

in which R is the gas constant, k is Boltzmann's constant, and γ_0 and γ_1 are the band parameters in the established notation. Actually, formula (38) is valid for $T << \gamma_1/k$ and (39) is valid for $T >> \gamma_1/k$; but in the vicinity of $T = \gamma_1/k$ the two formulas give almost equal values and it is sufficiently accurate to use each to $T = 0.73394\,\gamma_1/k$, at which temperature they give equal values.

Approved for Public Release

Contrails

McClure suggests that the best values for the band parameters for natural single-crystal graphite are

$$\gamma_0 = 2.8 \text{ eV} \quad \text{and} \quad \gamma_1 = 0.27 \text{ eV}. \tag{40}$$

With these values (38) and (39) reduce to

$$C_e = (2.27\,T + 3.74 \times 10^{-3}\,T^2 + 1.20 \times 10^{-6}\,T^3) \times 10^{-6} \text{ cal/mole °K} \quad \text{for } T \leq 2300 \text{ °K} \tag{41}$$

and

$$C_e = 7.48 \times 10^{-9}\,T^2 \text{ cal/mole °K} \quad \text{for } T \geq 2300 \text{ °K}, \tag{42}$$

in which T is in °K. The values of the electronic specific heat, computed from these formulas, are given in Table 3.

From measurements of the specific heat below 2°K, van der Hoeven and Keesom [28] find that the coefficient of the linear term is 3.30 for Madagascar single-crystal graphite and about 5 for fabricated graphites. It is beyond the scope of this work to investigate the cause of the difference between the values 2.27 and 3.30, or to investigate the electronic specific heat of the less-perfectly crystalline fabricated graphites at higher temperatures. For most temperatures the values given in Table 3 are sufficiently accurate. However, at very high temperatures an error of a factor of two in the electronic specific heat of fabricated graphite would be of interest in connection with the possibility that the lattice specific heat exceeds the Dulong and Petit value in this range.

2.5. Specific Heat C_t at Very High Temperatures

On measuring the specific heat of four grades of fabricated graphite Rasor and McClelland [27] found that between 3000°K and the sublimation temperature at about 3920°K the specific heat doubled in value. Their data indicated a thermally activated process with an activation energy of 7.7 ± .5 eV/atom. By fitting their data they arrived at the following formula for the contribution C_t to the specific heat of this thermal process:

$$C_t = 5.6 \times 10^{17}\,T^{-2} \exp(-8.9 \times 10^4/T) \text{ cal/mole °K}, \tag{43}$$

in which T is in °K. Values calculated from this equation are given in Table 3. Although the constants in (43) may not be exactly right for the average C_p curve used in this report, the agreement is close enough to confirm the general correctness of the form of equation (43).

Rasor and McClelland cite evidence both from their specific heat and from their thermal conductivity work that the mechanism of this process is the thermal creation of vacancies. In particular they note that the activation energy of 7.7 eV is close to the heat of sublimation 7.4 eV, which they take as approximately the energy of formation of a vacancy. However, recent electron

Approved for Public Release

Contrails

microscope studies of vacancy-controlled processes in graphite by Baker and Kelly[39] indicate that the energy of formation of a vacancy is only about 3.3 eV; so the interpretation of Rasor and McClelland's results in terms of vacancies is not completely certain.

2.6 Lattice Specific Heat

The specific heat at constant volume may be considered to be a function of the temperature and the volume. At atmospheric pressure the volume of the crystal is a unique function V(T) of the temperature, so one may write

$$C_v = C_v\ [\,T,\ V(T)\,].$$

However, theoretical calculations are usually based on the concept of a rigid lattice with lattice constants corresponding to some temperature T_0, which might be room temperature or 0°K. Thus, $C_v\ [\,T,\ V(T_0)\,]$ is of greater theoretical interest, and it is convenient to define a quantity E(T) by

$$E(T) = C_v\ [\,T,\ V(T)\,] - C_v\ [\,T,\ V(T_0)\,]. \tag{44}$$

The specific heat of the lattice vibrations of a rigid lattice, denoted by $C_\ell\,[\,T, V(T_0)\,]$ is even more fundamental and is given by

$$C_v\,[\,T, V(T_0)] = C_\ell\ [\,T,\ V(T_0)] + C_e\,[\,T,\ V(T_0)] + C_t\,[\,T,\ V(T_0)] \tag{45}$$

Combining equations (1), (44), and (45), we obtain for the lattice specific heat

$$C_\ell\ [\,T,\ V(\,T_0)] = C_p\,[\,T,\ V(T)] - V\beta^2 BT - C_e\,[\,T,\ V(T_0)] - C_t\,[\,T,\ V(T_0)\,] - E(T). \tag{46}$$

Overton[40] has shown how E(T) may be calculated from experimentally measured quantities. For sodium and copper, he found that E(T) was smaller than but not negligible compared to $V\beta^2 BT$. Since the data necessary to calculate E(T) are not available for graphite, this term must be neglected here.

The values of $C_\ell\ [\,T,\ V(T_0)]$ calculated by (46) are given in Table 3 for fabricated graphite. The results are not accurate enough for the precise value of T_0 to matter. The lattice specific heat exceeds the Dulong and Petit value of 5.96 cal/mole °K above about 2300°K. The experimental error ΔC and the approximations made in calculating C_ℓ from C_p are too large to draw any conclusions concerning the existence of anharmonic forces in graphite. The values of C_ℓ above 3000°K are not significant in that Rasor and McClelland had to assume a set of values for C_ℓ in this temperature range in order to derive their formula for C_t. The computed values of C_ℓ given in Table 3 indicate the approximate validity of formula (43) for C_t. Efforts to find analytic formulas to represent $C_\ell\,[\,T, V(T_0)]$ are described in the following section.

Approved for Public Release

Contrails

3. ANALYTICAL REPRESENTATION OF THE LATTICE SPECIFIC HEAT

3.1. Form of the Frequency Distributions in Graphite

In attempting to find an analytic function to best fit an empirical curve there are an endless number of functions which might be tried. To reduce the work to a reasonable amount certain rather arbitrary decisions have to be made at the beginning as to the types of functions to be considered. In making these decisions it is helpful to consider the general nature of the frequency distributions of the lattice vibrations in graphite and to review the results of the more rigorous Born-von Kármán type calculations.

There are 4 atoms in the unit cell of graphite, so there are 12 branches of the distribution of lattice vibration frequencies in reciprocal or wave-vector space. Because of lattice symmetry, the branches are degenerate across the top and bottom faces of the Brillouin zone, and it is more convenient to consider that there are 6 branches in a Brillouin zone which is twice as high. These 6 branches may be classified into 3 low-frequency acoustical modes and 3 high-frequency optical modes. Because of the weak interaction between layers, the directions of the atomic vibrations are mostly either parallel or perpendicular to the layer planes. This fact leads to a further classification of both the acoustical and optical modes as: "out-of-plane", "in-plane transverse" in which the vibrations are essentially in the layer plane and transverse to the direction of propagation, and "in-plane longitudinal" in which the vibrations are essentially in the layer planes and in the plane defined by the direction of propagation and its projection on the layer plane (a longitudinal wave only when the direction of propagation is in the layer plane).

The restoring forces for the "out-of-plane" modes are weaker than for the "in-plane" modes and, correspondingly, the frequency distributions for the "out-of-plane" modes occur at lower frequencies than do those of the "in-plane" modes. It appears from the Born-von Karman type calculations of Newell[41] Yoshimori and Kitano,[42] and Baldock[43] that the qualitative shape of the frequency distributions $N(\nu)$ is as shown in Figure 3.

3.2. Representation in Terms of Debye and Einstein Functions

From the shape of the distribution functions as given by Born-von Karman calculations and because of the approximate T^2 dependence of the specific heat at moderately low temperatures, it appears to be reasonable to represent the acoustical modes by two-dimensional Debye distributions for which the specific heat varies as T^2 at low temperatures. The optical modes should be reasonably well represented by rectangular or, if the distribution is narrow, by Einstein distributions. The rectangular distribution can be constructed from the difference of two one-dimensional Debye distributions. Although the specific heat of a one-dimensional Debye distribution varies as T at low temperatures, the two linear terms cancel in taking the difference of two functions, and the remainder is proportional to $\exp(-\Theta/T)$ at low temperatures, as is appropriate for optical modes. It should be noted that we are using one- and two-dimensional distributions only to approximate the true distributions and are not considering the graphite crystal as being either one or two dimensional.

Approved for Public Release

Contrails

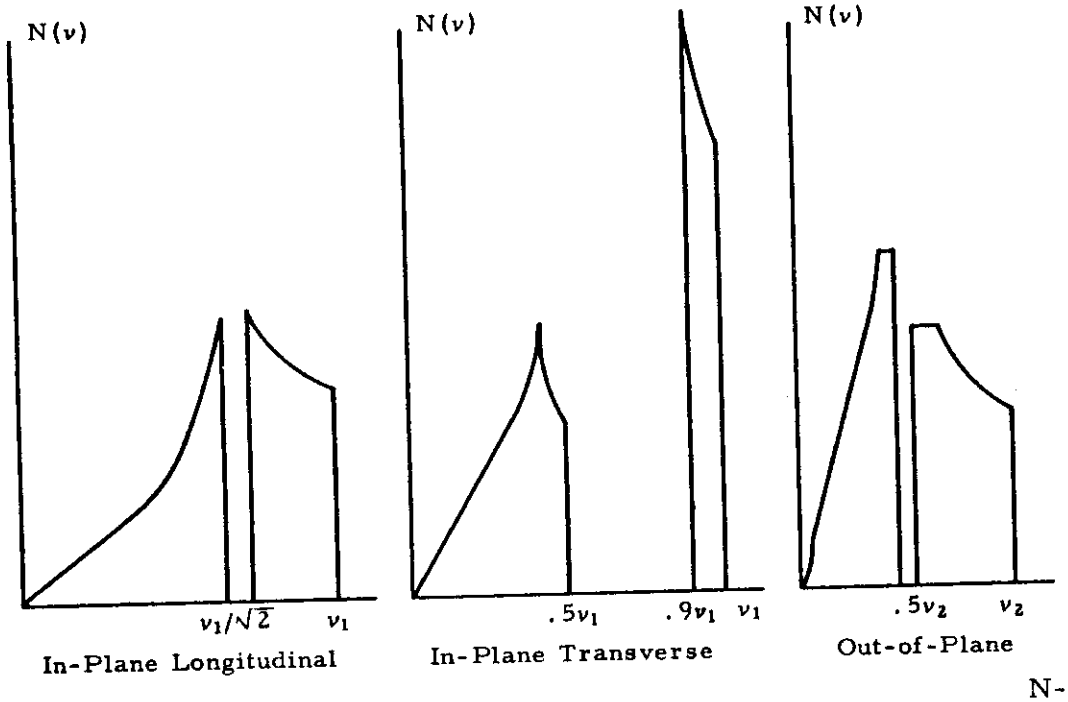

Figure 3. Qualitative Shape of the Frequency Distributions for Graphite

3.2.1. General Lattice Specific Heat Function

Let $N_j(\nu)$ be the frequency distribution of the jth branch ($j = 1, \cdots, 6$), normalized such that

$$\int_0^\infty N_j(\nu)\, d\nu = \tfrac{1}{2} N_0, \tag{47}$$

where N_0 is Avogadro's number. Also, let $D_1(x)$ and $D_2(x)$ be one- and two-dimensional Debye specific heat functions and $E(x)$ be the Einstein specific heat function, where

$$x = h\nu/kT. \tag{48}$$

Mathematical formulas and series expansions for these functions are given in the following section.

For the present purposes we wish to consider three types of distributions and their specific heat functions:

Approved for Public Release

Contrails

Linear

$$N_j(\nu) = N_0 \nu / \nu_j^2 \qquad \text{for } 0 \leq \nu \leq \nu_j \qquad (49)$$
$$= 0 \qquad \text{otherwise}$$

$$C_\ell(T) = \tfrac{1}{2} R D_2(x_j) \qquad (50)$$

Rectangular

$$N_j(\nu) = N_0/2(1-d_j)\nu_j \qquad \text{for } d_j\nu_j \leq \nu \leq \nu_j, \quad 0 \leq d_j < 1 \qquad (51)$$
$$= 0 \qquad \text{otherwise}$$

$$C_\ell(T) = [R/2(1-d_j)]\,[D_1(x_j) - d_j D_1(d_j x_j)] \qquad (52)$$

Einstein

$$N_j(\nu) = \tfrac{1}{2} N \delta(\nu - \nu_j) \qquad \delta = \text{Dirac delta function} \qquad (53)$$

$$C_\ell(T) = \tfrac{1}{2} R E(x_j). \qquad (54)$$

A computer program was prepared to compute the total lattice specific heat. Different types of functions could be chosen for the 6 branches by changing the input data. For a given choice of functions, the limiting frequencies were varied to obtain the best fit of the experimental curve. With the facilities available, it was impractical to vary more than three frequencies during the curve-fitting process. Therefore, the program was made to depend on only three characteristic frequencies or, equivalently, on three characteristic or Debye temperatures Θ_1, Θ_2, and Θ_3, where

$$\Theta_i = h\nu_i / k, \qquad i = 1, 2, 3. \qquad (55)$$

Thus, the specific heat of the jth branch depended on some $\Theta_{t(j)}$, where $t(j) = 1, 2,$ or 3. To allow flexibility the maximum frequency of each branch was taken to be some constant a_j times one of the three ν_i. The computer program computed the molar lattice specific heat from the formulas

$$C_\ell(T) = R \sum_{j=1}^{6} F_j(x_j), \qquad (56)$$

where

$$x_j = a_j \Theta_{t(j)} / T \qquad (57)$$

Approved for Public Release

Contrails

$$F_j(x_j) = f_j D_2(x_j) \qquad \text{for } j = 1, 2, \text{ and } 3 \tag{58}$$

$$F_j(x_j) = [f_j/(1-d_j)]\,[D_1(x_j) - d_j D_1(d_j x_j)] + e_j E(x_j) \qquad \text{for } j = 4, 5, \text{ and } 6 \tag{59}$$

and either $f_j = 0$ or $e_j = 0$ for $j = 4$, 5, and 6. The input data to the program consisted of the f's, e's, d's, a's, t's, Θ's, and a list of temperatures at which the value of C_ℓ was desired. The input data also contained the corresponding set of experimental values, which will now be denoted by C_ℓ^{exp}, from Table 3; and the program computed the difference

$$\text{Diff} = C_\ell(T) - C_\ell^{exp}(T). \tag{60}$$

The curve fitting was done by means of another program which computed a weighted mean square error MSE from

$$\text{MSE} = \frac{1}{n} \sum_{i=1}^{n} w_i \,[C_\ell(T_i) - C_\ell^{exp}(T_i)]^2, \tag{61}$$

where n is the number of temperatures used, w_i is a weighting factor included in the input data, and $C_\ell(T)$ is the value computed by equations (56) to (59). The input also included a set of increments $\Delta\Theta_i$ and the number of times $\Delta\Theta_i$ is to be added to Θ_i. The program computes MSE for the original Θ's, then increments one of the Θ's and recomputes MSE, etc. The output gives for each value of Θ_3 a matrix array of MSE values with the rows indexed by the values of Θ_1 and the columns indexed by the values of Θ_2. The procedure was to start with a coarse net of Θ values and find the general positions of the absolute and relative minima in the values of the mean square error. By repeating the calculations with smaller increments $\Delta\Theta$ the Θ values giving the minimum mean square error were found to the nearest 5 or 10 degrees, at which point the process was stopped.

The weighting of the mean square error was done implicitly by the choice of the temperatures used and explicitly by the choice of the weighting factors w_i. Perhaps the most logical choice of the weighting factors is the reciprocal of the square of the experimental error ΔC,

$$w_i = 1 / [\Delta C(T_i)]^2. \tag{62}$$

However, below 300°K the experimental curve is known so accurately that the weights given by (62) are overwhelmingly large; and in this region smaller weights had to be assigned on the basis of how close a fit is desired in this region. In order to reduce the computer time to a reasonable amount, only 7 temperatures were used. Since the primary objective is to obtain a reasonable fit over the entire temperature range, no effort was made to obtain an optimum fit in the T^2 region below 100°K. The values of T, C_ℓ^{exp}, and w_i used in the curve fitting are given in Table 7.

Approved for Public Release

Contrails

Table 7. Values of T, C_ℓ^{exp}, and w_i Used for Curve Fitting

T	C_ℓ^{exp}	w_i
100	0.400	2500
200	1.190	2500
300	2.061	2500
500	3.62	277
700	4.42	83
1000	5.01	69
1400	5.46	44

Units: T - °K; C_ℓ^{exp} - cal/mole °K;
w_i - mole^2 °K^2/cal^2

3.2.2. Formulas and Series Expansions for Debye and Einstein Functions

The Einstein specific heat function E(x) is defined by

$$E(x) = x^2 \, e^x / (e^x - 1)^2 . \tag{63}$$

For $x > 0.3$ the function E(x) was computed by (63) using the standard computer subroutine for the exponential function. For $x < 0.3$ the function

$$X(x) = x/(e^x - 1) \tag{64}$$

was computed from the expansion

$$x/(e^x - 1) = 1 - x/2 + \sum_{n=1}^{\infty} (-1)^{n-1} B_{2n-1} \, x^{2n}/(2n)! \quad , \tag{65}$$

where the B_{2n-1} are the Bernoulli numbers

$$B_1 = 1/6, \quad B_3 = 1/30, \quad B_5 = 1/42, \quad \text{etc.}; \tag{66}$$

and then E(x) was computed from

$$E(x) = X^2 \, e^x. \tag{67}$$

The one-dimensional Debye specific heat function is defined by

$$D_1(x) = \frac{2}{x} \int_0^x \frac{y \, dy}{e^y - 1} - \frac{x}{e^x - 1} \tag{68}$$

Approved for Public Release

Contrails

and the two-dimensional Debye specific heat function is defined by

$$D_2(x) = \frac{6}{x^2} \int_0^x \frac{y^2\, dy}{e^y - 1} - \frac{2x}{e^x - 1} \quad . \tag{69}$$

These functions were computed from series expansions derived in the same manner as Debye's [44] derivation of the series expansions of the original three-dimensional specific heat function.

For $x > 2$

$$D_1(x) = \frac{\pi^2}{3x} - \frac{2}{x} \sum_{n=1}^{\infty} \frac{(1+nx)\, e^{-nx}}{n^2} - \frac{x}{e^x - 1} \tag{70}$$

$$D_2(x) = \frac{12\zeta(3)}{x^2} - \frac{6}{x^2} \sum_{n=1}^{\infty} \frac{(2+2nx+n^2x^2)e^{-nx}}{n^3} - \frac{2x}{e^x - 1}\,, \tag{71}$$

where

$$\zeta(3) = 1.202056903.$$

For $x < 2$

$$D_1(x) = 1 - \sum_{n=1}^{\infty} \frac{(-1)^{n-1}\,(2n-1)\, B_{2n-1}\, x^{2n}}{(2n+1)\,!} \tag{72}$$

$$D_2(x) = 1 - \sum_{n=1}^{\infty} \frac{(-1)^{n-1}\,(2n-1)\, B_{2n-1}\, x^{2n}}{(n+1)\,(2n)\,!}\,, \tag{73}$$

where the B_{2n-1} are the Bernoulli numbers given by (66). Eight terms were used in each summation and the break point of $x = 2$ was chosen so that the two series expansion for D_1 and D_2 would have about the same accuracy at the break point. This procedure gives D_1 and D_2 correctly to 7 or more decimal places, which is rather more than adequate for the present study.

Approved for Public Release

Contrails

3.3. Numerical Examples

From 6 to 9 parameters a_j and d_j, depending on the choice of E(x) or D_1 (x) functions for the optical modes, had to be assigned initially to determine the general form of a frequency distribution. Then the specific form of the distribution was obtained by choosing the Θ's to minimize the mean square error. The program followed here was to start with a distribution whose general form approximated the more exact frequency distribution shown in Figure 3. Next, various simplifications in the general form were made to see if acceptable fits to the experimental curve could be obtained with simpler functions. Only a limited number of distributions could be examined within the contract period and the distributions reported here are not necessarily the best that could be found. Nevertheless, several distributions have been found that fit the experimental curve reasonably well and several points of general interest for the analytical representation of specific heat curves have arisen from this study.

Distribution A

The distribution tried initially was similar to that shown in Figure 4, except that the maximum frequency of the acoustical in-plane transverse mode was assigned the independent value ν_3. In order to save space the ordinates of the distributions shown in Figure 4 and subsequent figures have not been drawn to scale, and for convenience the abscissa has been labeled with the characteristic temperature instead of the frequency. It appeared from the calculations that the minimum mean square error MSE for this initial distribution would occur for ν_3 or, equivalently, Θ_3 greater than 0.9 Θ_1 ; that is, the acoustical and optical branches would overlap. This result was unexpected in that Figure 3 indicates that Θ_3 should be about 0.5 Θ_1 . At this point, it was decided to maintain some resemblance to the distributions of Figure 3 and a gap was arbitrarily set between the in-plane transverse distributions. The final result is the two-parameter distribution shown in Figure 4 and denoted

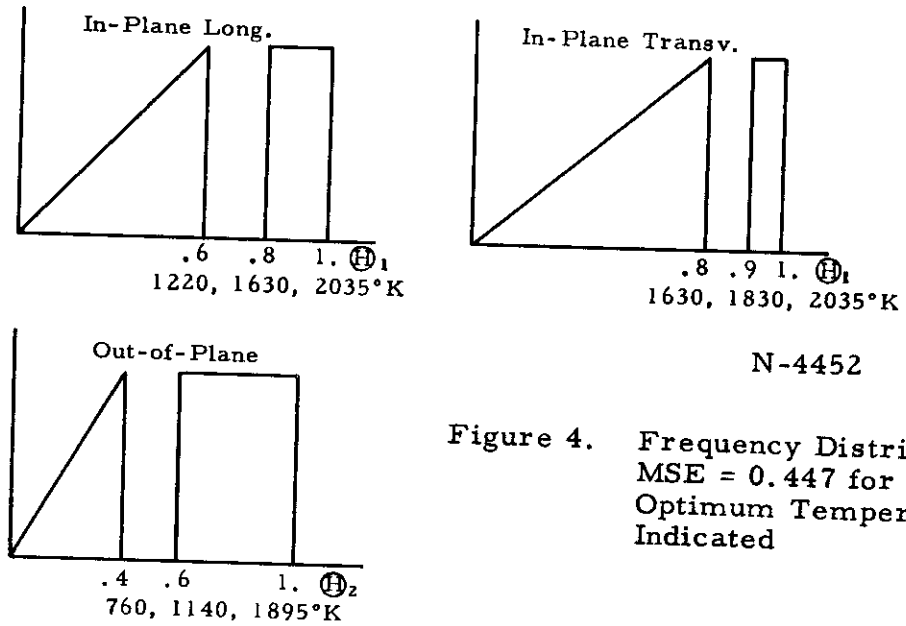

Figure 4. Frequency Distribution A. MSE = 0.447 for the Optimum Temperatures Indicated

Approved for Public Release

Contrails

by Distribution A. On carrying out the curve-fitting procedure with the temperatures and weights given in Table 7, the minimum mean square error was found to be MSE = 0.447 at Θ_1 = 2035°K and Θ_2 = 1895°K. From the definitions (61) and (62) of MSE and w_i it follows that for a mean square error of unity the computed curve is within the limits ΔC of the experimental curve on the average. However, because the computed and experimental curves cross each other several times, the difference between these curves may be several times ΔC in some regions, even when MSE = 1.

In order to see how sensitively the optimum characteristic temperatures depended on the choice of temperatures and weights used to fit the curve, Distribution A was refitted using 14 temperatures and larger weights which decreased from 15,625 at 100°K to 100 at 1200°K. The minimum mean square error with these larger weights was MSE = 0.805 at Θ_1 = 2045°K and Θ_2 = 1890°K. These values of Θ_1 and Θ_2 are in very good agreement with those found from the smaller set of 7 temperatures; so the smaller set, given in Table 7, was used for fitting all other distributions.

The lattice specific heat was computed from (56) using the optimum values Θ_1 = 2035°K and Θ_2 = 1895°K for a much larger set of temperatures. Table 8 gives the values of the functions $F_j(x_j)$ and $C_\ell(T)$ and of the difference Diff as defined by (60). The table was typed directly from the output tape of the computer; the number following the letter "E" is the power of ten by which the preceding decimal is to be multiplied, for example,

$$.48378E\text{-}05 = .48378 \times 10^{-5}.$$

From the column of Diff values it is seen that the computed and experimental curves cross each other five times. Below 200°K the magnitude of the difference between the curves is less than 0.03 cal/mole °K but the relative error is up to 20 per cent and even larger below 10°K, as expected. Above 200°K the relative error is about 2 per cent or less and the computed curve is within the experimental range $C_\ell^{exp} \pm \Delta C$ except around 400°K where it is within the range $C_\ell^{exp} \pm 2\,\Delta C$. Although the computed lattice specific heat for Distribution A is not the best that could be found, it should be a satisfactory approximation for most applications requiring an analytic specific heat function for the entire temperature range.

Distributions B,C, and D

The first step in simplifying Distribution A was to assume that the in-plane transverse modes have the same frequency distributions as the in-plane longitudinal modes. This approximation leads to Distribution B shown in Figure 5. The minimum MSE is 0.945 for Θ_1 = 2175°K and Θ_2 = 2035°K. The fit to the experimental curve is better at high temperatures but worse near and below room temperature, where the larger weighting factors cause a greater mean square error than for the curve for Distribution A.

Distributions C and D, shown in Figures 6 and 7, were tried to see the effect of shifting the position of the gap between the acoustical and optical out-of-plane modes. The minimum mean square errors are 1.56 and 1.97,

Approved for Public Release

Table 8. Lattice Specific Heat for Frequency Distribution A

T	$F_1(x_1)$	$F_2(x_2)$	$F_3(x_3)$	$F_4(x_4)$	$F_5(x_5)$	$F_6(x_6)$	$C_\ell(T)$	Diff
.10000E+01	.48378E-05	.27212E-05	.12553E-04	.00000E+00	.00000E+00	.00000E+00	.39961E-04	.27961E-04
.10000E+02	.48378E-03	.27212E-03	.12553E-02	.00000E+00	.00000E+00	.00000E+00	.39961E-02	.59610E-03
.20000E+02	.19351E-02	.10885E-02	.50211E-02	.00000E+00	.00000E+00	.00000E+00	.15984E-01	-.18156E-02
.30000E+02	.43540E-02	.24491E-02	.11297E-01	.00000E+00	.00000E+00	.00000E+00	.35965E-01	-.71351E-02
.40000E+02	.77404E-02	.43540E-02	.20084E-01	.00000E+00	.00000E+00	.00000E+00	.63937E-01	-.14863E-01
.50000E+02	.12094E-01	.68031E-02	.31377E-01	.00000E+00	.00000E+00	.00000E+00	.99893E-01	-.21107E-01
.60000E+02	.17416E-01	.97965E-02	.45137E-01	.00000E+00	.00000E+00	.74506E-07	.14376E+00	-.24245E-01
.70000E+02	.23705E-01	.13334E-01	.61222E-01	.00000E+00	.00000E+00	.12107E-05	.19524E+00	-.25758E-01
.80000E+02	.30957E-01	.17416E-01	.79326E-01	.74506E-07	.00000E+00	.82515E-05	.25375E+00	-.24251E-01
.90000E+02	.39164E-01	.22042E-01	.98989E-01	.55879E-06	.14901E-06	.36173E-04	.31837E+00	-.19627E-01
.10000E+03	.48299E-01	.27211E-01	.11967E+00	.30547E-05	.96858E-06	.11707E-03	.38804E+00	-.11955E-01
.12000E+03	.69137E-01	.39164E-01	.16192E+00	.38296E-04	.14305E-04	.66958E-03	.53835E+00	.33515E-02
.15000E+03	.10536E+00	.60948E-01	.22162E+00	.45385E-03	.22128E-03	.37108E-02	.77951E+00	.11513E-01
.20000E+03	.17060E+00	.10536E+00	.30049E+00	.48806E-02	.30400E-02	.19411E-01	.11997E+01	.96725E-02
.25000E+03	.23112E+00	.15435E+00	.35442E+00	.18661E-01	.13299E-01	.49687E-01	.16323E+01	.93453E-02
.30000E+03	.28153E+00	.20196E+00	.39074E+00	.43088E-01	.33391E-01	.89470E-01	.20668E+01	.57788E-02
.35000E+03	.32159E+00	.24473E+00	.41568E+00	.75258E-01	.61691E-01	.13246E+00	.24865E+01	-.13507E-01
.40000E+03	.35293E+00	.28153E+00	.43327E+00	.11113E+00	.94785E-01	.17425E+00	.28769E+01	-.53083E-01
.45000E+03	.37743E+00	.31247E+00	.44604E+00	.14744E+00	.12946E+00	.21257E+00	.32296E+01	-.70385E-01
.50000E+03	.39671E+00	.33823E+00	.45555E+00	.18210E+00	.16343E+00	.24657E+00	.35419E+01	-.78077E-01
.55000E+03	.41202E+00	.35963E+00	.46280E+00	.21405E+00	.19537E+00	.27619E+00	.38151E+01	-.84943E-01
.60000E+03	.42432E+00	.37743E+00	.46844E+00	.24285E+00	.22463E+00	.30177E+00	.40523E+01	-.17715E-01
.65000E+03	.43431E+00	.39230E+00	.47290E+00	.26851E+00	.25102E+00	.32378E+00	.42577E+01	.76909E-02
.70000E+03	.44251E+00	.40479E+00	.47649E+00	.29120E+00	.27459E+00	.34272E+00	.44355E+01	.15457E-01
.75000E+03	.44930E+00	.41535E+00	.47942E+00	.31119E+00	.29553E+00	.35903E+00	.45895E+01	.29489E-01
.80000E+03	.45499E+00	.42432E+00	.48184E+00	.32878E+00	.31409E+00	.37312E+00	.47233E+01	.33268E-01
.85000E+03	.45980E+00	.43200E+00	.48386E+00	.34428E+00	.33053E+00	.38533E+00	.48398E+01	.49810E-01
.90000E+03	.46389E+00	.43860E+00	.48556E+00	.35795E+00	.34510E+00	.39597E+00	.49417E+01	.61680E-01
.95000E+03	.46739E+00	.44432E+00	.48701E+00	.37003E+00	.35803E+00	.40527E+00	.50311E+01	.81059E-01
.10000E+04	.47042E+00	.44930E+00	.48826E+00	.38073E+00	.36953E+00	.41342E+00	.51098E+01	.99767E-01
.11000E+04	.47535E+00	.45749E+00	.49026E+00	.39873E+00	.38894E+00	.42698E+00	.52411E+01	.10108E+00
.12000E+04	.47915E+00	.46389E+00	.49180E+00	.41310E+00	.40453E+00	.43767E+00	.53452E+01	.85168E-01
.13000E+04	.48215E+00	.46896E+00	.49300E+00	.42473E+00	.41717E+00	.44623E+00	.54288E+01	.68825E-01
.14000E+04	.48455E+00	.47305E+00	.49395E+00	.43424E+00	.42755E+00	.45318E+00	.54969E+01	.36921E-01
.15000E+04	.48649E+00	.47639E+00	.49472E+00	.44210E+00	.43614E+00	.45889E+00	.55530E+01	.12999E-01
.16000E+04	.48810E+00	.47915E+00	.49536E+00	.44866E+00	.44333E+00	.46363E+00	.55997E+01	-.20327E-01
.17000E+04	.48943E+00	.48146E+00	.49589E+00	.45418E+00	.44940E+00	.46760E+00	.56389E+01	-.41102E-01
.18000E+04	.49056E+00	.48341E+00	.49633E+00	.45888E+00	.45456E+00	.47097E+00	.56722E+01	-.67847E-01
.19000E+04	.49151E+00	.48507E+00	.49670E+00	.46290E+00	.45898E+00	.47384E+00	.57006E+01	-.99426E-01
.20000E+04	.49233E+00	.48649E+00	.49702E+00	.46637E+00	.46279E+00	.47632E+00	.57250E+01	-.12496E+00
.22000E+04	.49365E+00	.48880E+00	.49754E+00	.47200E+00	.46901E+00	.48032E+00	.57648E+01	-.17524E+00
.24000E+04	.49465E+00	.49056E+00	.49793E+00	.47634E+00	.47380E+00	.48340E+00	.57953E+01	-.16556E+00
.26000E+04	.49544E+00	.49194E+00	.49823E+00	.47975E+00	.47757E+00	.48581E+00	.58193E+01	-.14159E+00
.28000E+04	.49606E+00	.49304E+00	.49848E+00	.48248E+00	.48059E+00	.48773E+00	.58384E+01	-.12245E+00
.30000E+04	.49657E+00	.49392E+00	.49867E+00	.48470E+00	.48304E+00	.48929E+00	.58539E+01	-.10692E+00
.32000E+04	.49698E+00	.49465E+00	.49883E+00	.48652E+00	.48505E+00	.49057E+00	.58667E+01	-.94155E-01
.34000E+04	.49732E+00	.49526E+00	.49897E+00	.48804E+00	.48673E+00	.49164E+00	.58773E+01	-.83540E-01
.36000E+04	.49761E+00	.49577E+00	.49908E+00	.48931E+00	.48815E+00	.49253E+00	.58862E+01	-.74616E-01
.38000E+04	.49786E+00	.49620E+00	.49917E+00	.49040E+00	.48934E+00	.49329E+00	.58938E+01	-.67046E-01
.40000E+04	.49806E+00	.49657E+00	.49925E+00	.49132E+00	.49037E+00	.49394E+00	.59003E+01	-.60568E-01

Approved for Public Release

Contents

Contrails

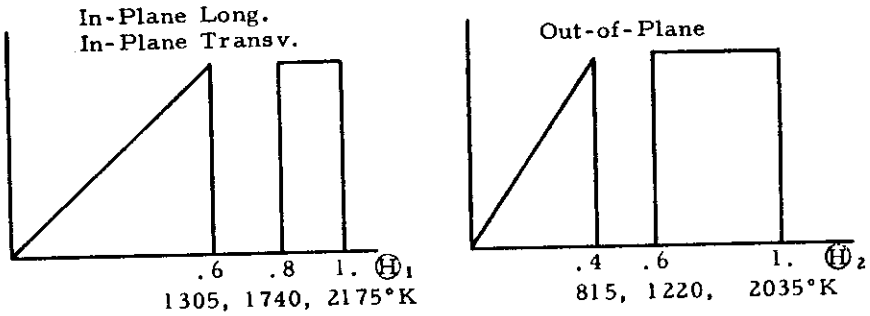

Figure 5. Frequency Distribution B. MSE = 0.945 for the Optimum Temperatures Indicated

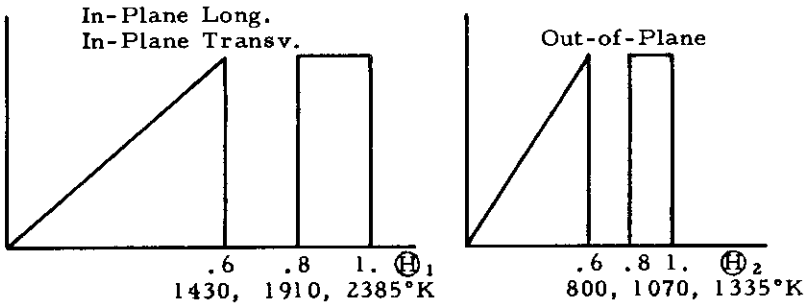

Figure 6. Frequency Distribution C. MSE = 1.56 for the Optimum Temperatures Indicated

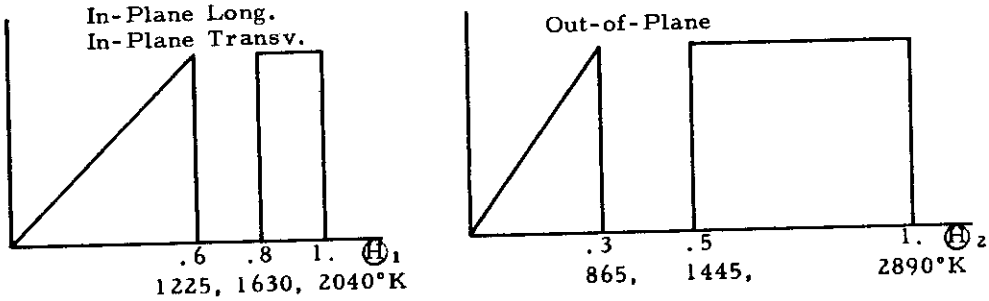

N-4451

Figure 7. Frequency Distribution D. MSE = 1.97 for the Optimum Temperatures Indicated

Approved for Public Release

Contrails

respectively, and the fit to the experimental curve is appreciably worse below 500°K than for Distribution A. Below room temperature, about 85 per cent of the specific heat is due to the acoustical modes. Since the curve-fitting procedure has emphasized this temperature range, it is not surprising to find that the average characteristic temperature of the in-plane acoustical modes is about 1300 ± 100°K and that of the out-of-plane acoustical mode is about 800 ± 100°K for all four distributions, A through D. On the other hand, the upper characteristic temperatures of the optical modes vary by several hundred degrees and cannot be accurately determined from the present experimental data.

Distribution E

In several theoretical calculations the four in-plane modes have been represented by a single Debye function. Distribution E, shown in Figure 8, has been investigated to see the effect of the approximation of neglecting the optical modes or, more accurately, of assuming that the optical and acoustical modes have the same frequency distribution. Surprisingly, this distribution gave the best fit of all. The minimum mean square error is only MSE = 0.289 for Θ_1 = 2165°K and Θ_2 = 1735°K. The good fit must be considered as fortuitous, since there is no theoretical justification for treating the optical modes in this manner.

It has been claimed in fitting a distribution such as Distribution E to the experimental data that the low temperature specific heat is due almost entirely to the acoustical out-of-plane mode and that its characteristic temperature (695°K in this case) can be determined from the low temperature data by neglecting the in-plane modes entirely. This is not the case. In spite of the high characteristic temperature of 2165°K of the four in-plane modes of Distribution E, these modes contribute about one third of the specific heat at all temperatures below 100°K.

Distribution F

The simplest frequency distribution investigated here is based on the approximation of assuming that all optical and acoustical modes have the same form. This approximation results in Distribution F, shown in Figure 9. The minimum mean square error is MSE = 2.14 at Θ_1 = 2450°K and Θ_2 = 1070°K. Table 9, which is similar to Table 8, gives the computed lattice specific heat, Diff, $F_1(x_1)$ and $F_3(x_3)$ for several temperatures for Distribution F. The fit to the experimental curve at high temperatures is as good as for any distribution investigated but the fit below 150°K is worse. As is to be expected the fit below 150°K using the two two-dimensional Debye functions of Distribution F is much better than the fit obtained by Magnus using two three-dimensional Debye functions. For example, at 40°K Magnus' formula[9] gives C_v = 0.024, compared to 0.055 for Distribution F. The experimental value is 0.079 ± .002 cal/mole °K.

An upper characteristic temperature for the in-plane modes of around 2500°K has often been quoted in the literature. Although a value in this range

Approved for Public Release

Contrails

Table 9. Lattice Specific Heat for Frequency Distribution F

T	$F_1(x_1)$	$F_2(x_2)$	$F_3(x_3)$	$F_4(x_4)$	$F_5(x_5)$	$F_6(x_6)$	$C_f(T)$	Diff
.10000E+01	.48062E-05	.00000E+00	.12599E-04	.00000E+00	.00000E+00	.00000E+00	.34583E-04	.22583E-04
.10000E+02	.48062E-03	.00000E+00	.12599E-02	.00000E+00	.00000E+00	.00000E+00	.34583E-02	.58346E-04
.20000E+02	.19225E-02	.00000E+00	.50396E-02	.00000E+00	.00000E+00	.00000E+00	.13833E-01	-.39666E-02
.30000E+02	.43256E-02	.00000E+00	.11339E-01	.00000E+00	.00000E+00	.00000E+00	.31125E-01	-.11975E-01
.40000E+02	.76900E-02	.00000E+00	.20159E-01	.00000E+00	.00000E+00	.00000E+00	.55334E-01	-.23466E-01
.50000E+02	.12016E-01	.00000E+00	.31498E-01	.00000E+00	.00000E+00	.00000E+00	.86459E-01	-.34541E-01
.60000E+02	.17302E-01	.00000E+00	.45356E-01	.00000E+00	.00000E+00	.00000E+00	.12450E+00	-.45501E-01
.70000E+02	.23551E-01	.00000E+00	.61727E-01	.00000E+00	.00000E+00	.00000E+00	.16944E+00	-.51558E-01
.80000E+02	.30760E-01	.00000E+00	.80582E-01	.00000E+00	.00000E+00	.00000E+00	.22123E+00	-.56770E-01
.90000E+02	.38930E-01	.00000E+00	.10184E+00	.00000E+00	.00000E+00	.00000E+00	.27970E+00	-.57895E-01
.10000E+03	.48062E-01	.00000E+00	.12535E+00	.00000E+00	.00000E+00	.00000E+00	.34455E+00	-.55448E-01
.12000E+03	.69210E-01	.00000E+00	.17803E+00	.00000E+00	.00000E+00	.00000E+00	.49125E+00	-.43750E-01
.15000E+03	.10813E+00	.00000E+00	.26576E+00	.00000E+00	.00000E+00	.00000E+00	.74291E+00	-.25085E-01
.20000E+03	.19195E+00	.00000E+00	.41170E+00	.00000E+00	.00000E+00	.00000E+00	.11994E+01	.94248E-02
.25000E+03	.29740E+00	.00000E+00	.53562E+00	.00000E+00	.00000E+00	.00000E+00	.16552E+01	.32168E-01
.30000E+03	.41894E+00	.00000E+00	.63213E+00	.00000E+00	.00000E+00	.00000E+00	.20881E+01	.27425E-01
.35000E+03	.54869E+00	.00000E+00	.70519E+00	.00000E+00	.00000E+00	.00000E+00	.24911E+01	-.86045E-02
.40000E+03	.67903E+00	.00000E+00	.76036E+00	.00000E+00	.00000E+00	.00000E+00	.28600E+01	-.70003E-01
.45000E+03	.80425E+00	.00000E+00	.80293E+00	.00000E+00	.00000E+00	.00000E+00	.31923E+01	-.10772E+00
.50000E+03	.92082E+00	.00000E+00	.83473E+00	.00000E+00	.00000E+00	.00000E+00	.34833E+01	-.13167E+00
.55000E+03	.10271E+01	.00000E+00	.86017E+00	.00000E+00	.00000E+00	.00000E+00	.37499E+01	-.11014E+00
.60000E+03	.11226E+01	.00000E+00	.88032E+00	.00000E+00	.00000E+00	.00000E+00	.39796E+01	-.90350E-01
.65000E+03	.12077E+01	.00000E+00	.89653E+00	.00000E+00	.00000E+00	.00000E+00	.41810E+01	-.69050E-01
.70000E+03	.12831E+01	.00000E+00	.90973E+00	.00000E+00	.00000E+00	.00000E+00	.43571E+01	-.62891E-01
.75000E+03	.13499E+01	.00000E+00	.92062E+00	.00000E+00	.00000E+00	.00000E+00	.45113E+01	-.48677E-01
.80000E+03	.14088E+01	.00000E+00	.92968E+00	.00000E+00	.00000E+00	.00000E+00	.46465E+01	-.43180E-01
.85000E+03	.15072E+01	.00000E+00	.93730E+00	.00000E+00	.00000E+00	.00000E+00	.47653E+01	-.24712E-01
.90000E+03	.15481E+01	.00000E+00	.94377E+00	.00000E+00	.00000E+00	.00000E+00	.48699E+01	-.10109E-01
.95000E+03	.15846E+01	.00000E+00	.94930E+00	.00000E+00	.00000E+00	.00000E+00	.49623E+01	.12287E-01
.10000E+04	.16461E+01	.00000E+00	.95406E+00	.00000E+00	.00000E+00	.00000E+00	.50441E+01	.34143E-01
.11000E+04	.16955E+01	.00000E+00	.96179E+00	.00000E+00	.00000E+00	.00000E+00	.51817E+01	.41749E-01
.12000E+04	.17357E+01	.00000E+00	.96773E+00	.00000E+00	.00000E+00	.00000E+00	.52913E+01	.31781E-01
.13000E+04	.17687E+01	.00000E+00	.97240E+00	.00000E+00	.00000E+00	.00000E+00	.53803E+01	.20840E-01
.14000E+04	.17960E+01	.00000E+00	.97613E+00	.00000E+00	.00000E+00	.00000E+00	.54537E+01	-.62504E-02
.15000E+04	.18189E+01	.00000E+00	.97915E+00	.00000E+00	.00000E+00	.00000E+00	.55141E+01	-.25922E-01
.16000E+04	.18382E+01	.00000E+00	.98164E+00	.00000E+00	.00000E+00	.00000E+00	.55645E+01	-.55512E-01
.17000E+04	.18546E+01	.00000E+00	.98371E+00	.00000E+00	.00000E+00	.00000E+00	.56070E+01	-.73007E-01
.18000E+04	.18688E+01	.00000E+00	.98545E+00	.00000E+00	.00000E+00	.00000E+00	.56431E+01	-.98869E-01
.19000E+04	.18809E+01	.00000E+00	.98692E+00	.00000E+00	.00000E+00	.00000E+00	.56741E+01	-.12591E+00
.20000E+04	.18913E+01	.00000E+00	.98819E+00	.00000E+00	.00000E+00	.00000E+00	.57008E+01	-.14220E+00
.22000E+04	.19003E+01	.00000E+00	.99022E+00	.00000E+00	.00000E+00	.00000E+00	.57443E+01	-.19574E+00
.24000E+04	.19161E+01	.00000E+00	.99177E+00	.00000E+00	.00000E+00	.00000E+00	.57778E+01	-.18308E+00
.26000E+04	.19281E+01	.00000E+00	.99298E+00	.00000E+00	.00000E+00	.00000E+00	.58041E+01	-.15673E+00
.28000E+04	.19378E+01	.00000E+00	.99394E+00	.00000E+00	.00000E+00	.00000E+00	.58252E+01	-.13564E+00
.30000E+04	.19456E+01	.00000E+00	.99472E+00	.00000E+00	.00000E+00	.00000E+00	.58423E+01	-.11851E+00
.32000E+04	.19521E+01	.00000E+00	.99536E+00	.00000E+00	.00000E+00	.00000E+00	.58564E+01	-.10442E+00
.34000E+04	.19575E+01	.00000E+00	.99589E+00	.00000E+00	.00000E+00	.00000E+00	.58682E+01	-.92684E-01
.36000E+04	.19620E+01	.00000E+00	.99633E+00	.00000E+00	.00000E+00	.00000E+00	.58780E+01	-.82814E-01
.38000E+04	.19658E+01	.00000E+00	.99671E+00	.00000E+00	.00000E+00	.00000E+00	.58864E+01	-.74434E-01
.40000E+04	.19691E+01	.00000E+00	.99703E+00	.00000E+00	.00000E+00	.00000E+00	.58936E+01	-.67260E-01

Approved for Public Release

Contrails

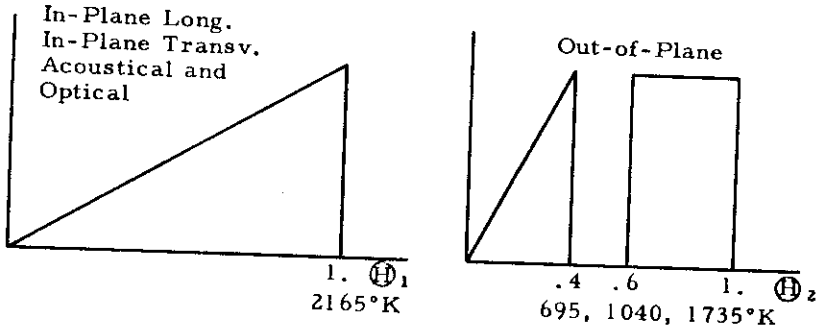

Figure 8. Frequency Distribution E. MSE = 0.289 for the Optimum Temperatures Indicated

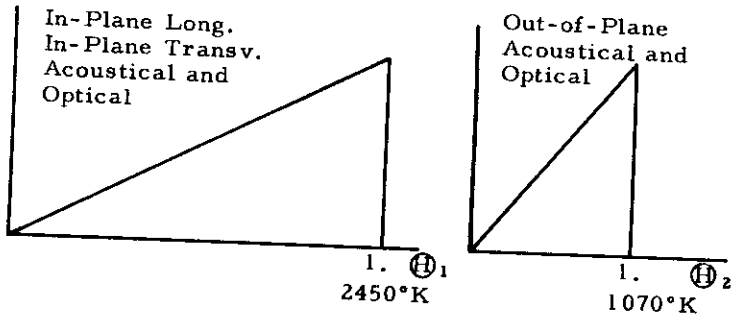

Figure 9. Frequency Distribution F. MSE = 2.14 for the Optimum Temperatures Indicated

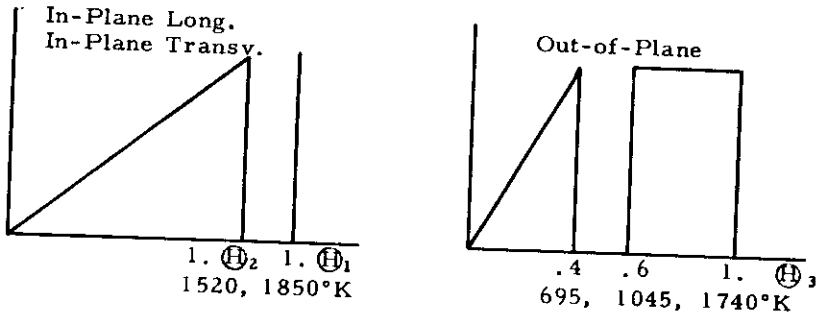

Figure 10. Frequency Distribution G. MSE = 0.292 for the Optimum Temperatures Indicated

N-4450

Approved for Public Release

Contrails

was obtained for Distribution F, all the other distributions give values closer to 2000°K. It seems likely that very little significance should be given to the upper characteristic temperature until the shape of the optical modes has been determined more accurately.

Distribution G

The narrowness of the distributions of the in-plane optical modes of Distributions A and B suggests that these distributions could be approximated by Einstein distributions at a single frequency. This point is illustrated by Distribution G, shown in Figure 10, which has three independent characteristic temperatures. Probably because the minimization was carried out with respect to three Θ's, a good fit was obtained for Distribution G, the minimum mean square error being MSE = 0.292 for the optimum temperatures shown in Figure 10. The computed and experimental curves cross seven times and the fit is particularly good in the room temperature region.

One point may be noted which applies to all distributions. Since the mean square error is a function of Θ_1 and Θ_2, it can be plotted as a surface above the Θ_1 Θ_2-plane. This surface has a single valley with rather steep sides. The bottom of the valley has a very gentle slope and usually has one relative minimum and one absolute minimum. If Θ_1 and Θ_2 are changed from their optimum values in such a way as to stay along the bottom of the valley, then rather large changes can be made in Θ_1 and Θ_2 with only a small increase in the mean square error. These points are illustrated for Distribution C by the values of MSE given in Table 10. For example, the effect of a 35°K change in Θ_1 (2385 to 2350) can be canceled by a change of 25°K in Θ_2 (1335 to 1360), thereby producing a fit which is essentially as good as the optimum. The gentle slope of the bottom of the valley seems to explain the equal success of elaborate calculations based on very different models of atomic forces but which have a parameter that is arbitrarily varied until the MSE is in the bottom of the valley. A good fit does not necessarily confirm the correctness of the rest of the calculation.

Table 10. Mean Square Errors for Frequency Distribution C

Θ_1 °K	Θ_2 °K	MSE	Type of Point
2500	1250	1.92	Bottom
2350	1360	1.58	Bottom
2350	1335	1.87	Side
2385	1335	1.56	Abs. Min.
2385	1360	1.81	Side
~1950	~1850	3.32	Saddle
~1625	~2900	~2.0	Rel. Min.

Approved for Public Release

Contrails

4. SUMMARY AND CONCLUSIONS

Several conclusions can be drawn from the results of the literature survey of the experimental measurements of the specific heat of graphite. Also, the survey indicates the need for additional experimental data in several areas.

For engineering purposes, it appears that the specific heat of all coke-base graphites is the same at all temperatures and that the average specific heat curve is adequately known below about 2000°K. Above 2000°K all the reliable data were taken on the same experimental equipment; and some additional measurements are desirable in this range, particularly of the rapid increase in the specific heat above 3000°K.

For scientific purposes, the data are less satisfactory. The specific heat of lampblack-based graphite, which has been measured only below 20°K, should be measured at higher temperatures. This data would provide a more complete check on theories which account for the increase in the specific heat of this type of graphite in terms of changes in the elastic stiffness constants c_{33} and c_{44}. There does not appear to be any very accurate (± 1 per cent) measurements of the specific heat of any type of graphite in the range of a few hundred degrees above room temperature. The apparent difference between the specific heats of natural and coke-based graphite below room temperature should be investigated above room temperature.

There is a need for more accurate data on the difference between the specific heat at constant pressure and at constant volume. At present there are no measurements of the temperature dependence of the bulk modulus of graphite crystals. Accurate values over a temperature interval of even a few hundred degrees would be valuable for checking the estimate of the temperature dependence made in this study. There does not appear to be accurate data on the crystallite coefficient of thermal expansion along the c-axis of coke-based and lampblack-based graphites in the region of a few hundred degrees below and above room temperature, although some data exist at higher temperatures. Until the C_p-C_v term is accurately known, the theoretically interesting question of an anelastic component in the lattice specific heat cannot be answered.

It was found that combinations of Einstein and one- and two-dimensional Debye functions could be found which both adequately approximated the lattice specific heat curve and roughly approximated the frequency distributions for the acoustical and optical modes. However, it was found that an equally good fit to the experimental curve could be obtained by a distribution which did not properly treat the optical in-plane modes. This result appears to be fortuitous and the additional neglect of the optical out-of-plane mode gave a poor fit. The use of two-dimensional Debye functions for the acoustical modes seems to be definitely better than the use of three-dimensional functions at temperatures below 150°K, but the large experimental uncertainty at temperatures above 500°K makes it difficult to choose between two- and three-dimensional functions in this region. Rather different sets of characteristic temperatures

Approved for Public Release

Contrails

(Θ_1, Θ_2) or (Θ_1, Θ_2, Θ_3) could be found that gave essentially equal fits to the experimental curve. Because of this and because very different models of the frequency distributions gave nearly the same result, it is not possible to determine unique characteristic temperatures. However, it appears that the highest frequency for which there is a significant number of in-plane optical modes corresponds to a temperature closer to 2000°K than to the often used 2500°K. The characteristic temperature of the acoustical out-of-plane mode represented by a two-dimensional Debye function is in the range 755 ± 60°K for the models which gave good approximations to the experimental curve.

Approved for Public Release

Contrails

REFERENCES

1. D. D. Wagman, J. E. Kilpatrick, W. J. Taylor, K. S. Pitzer, and F. D. Rossini, J. Research Nat. Bur. Standards 34, 143 (1945).

2. F. G. Brickwedde, M. Moskow, and J. G. Aston, J. Research Nat. Bur. Standards 37, 263 (1946).

3. F. D. Rossini, K. S. Pitzer, R. L. Arnett, R. M. Braun, G. C. Pimentel, et. al., Selected Values of Physical and Thermodynamic Properties of Hydrocarbons and Related Compounds, Carnegie Inst. Tech., 1953, (Am. Pet. Inst. Res. Proj. 44).

4. T. C. Goodwin, Jr., and M. W. Ayton, U. S. Wright Air Development Center, WADC Tech. Rept. 56-423 (Aug., 1956).

5. V. J. Johnson, ed., A Compendium of the Properties of Materials at Low Temperatures, Phase I, U. S. Nat. Bur. Standards Cryogenic Eng. Lab., Final Rept. to U. S. Wright Air Development Center on Contract No. (33-616) 58-4 (Dec., 1959).

6. U. S. Nat. Bur. Standards, Preliminary Report on the Thermodynamic Properties of Selected Light - Element Compounds, NBS Report 6928 (July, 1960).

7. K. K. Kelley, Contributions to the Data on Theoretical Metallurgy - XIII, U. S. Bur. Mines Bull. 584 (1960).

8. K. K. Kelley and E. G. King, ibid - XIV, U. S. Bur. Mines Bull. 592 (1961).

9. A. Magnus, Ann. Physik 70, 303 (1923).

10. J. Krumhansl and H. Brooks, J. Chem. Phys. 21, 1663 (1953).

11. J. C. Bowman and J. A. Krumhansl, J. Phys. Chem. Solids 6, 367 (1958) and references therein.

12. V. V. Tarasov, Akad. Nauk S.S.S.R. 10, 136 (1954) and references therein.

13. W. DeSorbo, J. Am. Chem. Soc. 77, 4713 (1955).

14. W. DeSorbo and W. W. Tyler, J. Chem. Phys. 21, 1660 (1953).

15. U. Bergenlid, R. W. Hill, F. J. Webb, and J. Wilks, Phil. Mag. 45, 851 (1954).

16. I. Estermann and G. I. Kirkland, Carnegie Inst. Tech. Rept. CC-3161, Rn-Cr, Contract W-7405-eng-277, "A" Rept. No. 13 (Sept. 1945). Unclassified.

Approved for Public Release

Contrails

17. C. J. Jacobs and G. S. Parks, J. Am. Chem. Soc. 56, 1513 (1934).

18. W. Nernst, Ann. Physik 36, 395 (1911).

19. F. Koref, Ann. Physik 36, 49 (1911).

20. H. F. Weber, Pogg. Ann. 154, 367 (1875), as corrected by Magnus, Reference 9.

21. P. Schlapfer and P. Debrunner, Helv. Chim. Acta 7, 31 (1924).

22. C. F. Lucks and H. W. Deem, U. S. Wright Air Development Center WADC Tech. Rept. 55-496 (Aug., 1956) and C. F. Lucks, H. W. Deem, and W. D. Wood, Am. Ceramic Soc. Bull. 39, 313 (1960).

23. D. S. Neel, C. D. Pears, and S. Oglesby, Jr., U. S. Wright Air Development Division WADD Tech. Rept. 60-924 (Nov., 1960).

24. I. B. Fieldhouse, J. I. Lang, and H. H. Blau, U. S. Wright Air Development Division WADC Tech. Rept. 59-744, Vol. IV (Oct., 1960).

25. I. B. Fieldhouse, J. C. Hedge, J. I. Lang, A. N. Takata and T. E. Waterman, U. S. Wright Air Development Center WADC Tech. Rept. 55-495, Part I (Sept., 1956).

26. A. G. Worthing, Phys. Rev. 12, 199 (1918).

27. N. S. Rasor and J. D. McClelland, U. S. Wright Air Development Center WADC Tech. Rept. 56-400, Part I (Mar., 1957) and J. Phys. Chem. Solids 15, 17 (1960).

28. B. J. C. van der Hoeven, Jr., and P. H. Keesom, Phys. Rev. 130, 1318 (1963) and references therein.

29. J. B. Nelson and D. P. Riley, Proc. Phys. Soc. 57, 477 (1945) and D. P. Riley, Proc. Phys. Soc. 57, 486 (1945).

30. P. L. Walker, Jr., and C. C. Wright, Ind. and Eng. Chem. 45, 1711 (1953).

31. Y. Baskin and L. Meyer, Phys. Rev. 100, 544 (1955).

32. E. Matuyama, J. Sci. Instr. 32, 229 (1955) and Chem. Abs. 53, 14629i (1959) [Tanso 7, 12 (1958)].

33. E. G. Steward and B. P. Cook, Nature 185, 78 (1960).

34. E. G. Steward, B. P. Cook, and E. A. Kellett, Nature 187, 1015 (1960).

Approved for Public Release

Contrails

35. C. E. Lowell, WADD Tech. Rept. 61-72, Vol. XXIV (1963), The Thermal Expansion of Graphite in the C_0 Direction.

36. P. W. Bridgman, Proc. Am. Acad. Arts and Sci. 76, 9 (1945) and 76, 55 (1948).

37. S. S. Kabalkina and L. F. Vereshchagin, Soviet Phys. - Doklady 5, 373 (1960); Doklady Akad. Nauk S.S.S.R. 131, 300 (1960).

38. K. Komatsu and T. Nagamiya, J. Phys. Soc. (Japan) 6, 438 (1951).

39. C. Baker and A. Kelly, Nature 193, 235 (1962).

40. W. C. Overton, Jr., J. Chem. Phys. 37, 2975 (1962).

41. G. F. Newell, J. Chem. Phys. 24, 1049 (1956) and 27, 240 (1957).

42. A. Yoshimori and Y. Kitano, J. Phys. Soc. (Japan) 11, 352 (1956).

43. G. R. Baldock, Phil. Mag. 1, 789 (1956).

44. P. Debye, Ann. Physik 39, 789 (1912).

Approved for Public Release

Contrails

Approved for Public Release

Contrails

Approved for Public Release